Advanced Research Projects Agency
Office of the Director of Defense Research and Engineering

Principles of Atmospheric Reentry

by Theodore A. George

NOVEMBER 1961

PRINCIPLES OF ATMOSPHERIC REENTRY

By

Theodore A. George

* * *

Advanced Research Projects Agency
Office of the Director of Defense Research and Engineering
Washington 25, D. C.

November 1961

CONTENTS

ABSTRACT

This paper summarizes the entire field of a space vehicle's reentry into the earth's atmosphere. It is assumed that the vehicle, either lifting or nonlifting, is approaching the earth from outer space and must pass through all densities of the atmosphere from $\rho = 0$ as it enters at high altitude until it lands at approximately sea level or $\rho = \rho_{SL}$ (that is, ρ_{MAX}).

During the vehicle's descent through the earth's atmosphere, deceleration must not exceed a maximum value, the total heat taken in by the vehicle must not be excessive, and the vehicle's skin or internal temperature must be limited. Methods of attaining these objectives are explained.

1. INTRODUCTION

The purposes of this paper are (1) to review, consolidate and, where appropriate, summarize available knowledge affecting the behavior of a body entering the earth's atmosphere at a high velocity and (2) to indicate how the difficulties encountered during such a flight can be overcome. It must be emphasized, therefore, that this is not merely a summary of various technical papers on reentry but is rather an effort to present the entire subject in a single cohesive treatise that bridges existing gaps between the related disciplines.

From a practical standpoint, this field of research has been concerned primarily with man-made objects (vehicles) in their plunge back into the earth's atmosphere; hence, the word "reentry" is usually associated with the subject. In January 1959, when this paper was begun, there was no single text to which a reader could refer for a general understanding of the complex field of atmospheric reentry. There were a large number of papers touching on certain specialized aspects of reentry, and most of these presupposed that the reader had a considerable background and understanding of the technical field covered. This situation made it very hard for the average engineer to obtain a broad view of reentry technology in a short time. Also, specialists working in the other areas of space technology--propulsion, communications, celestial mechanics--frequently need a dependable reference on reentry when their work overlaps that field. This paper attempts to satisfy these requirements; also, an exhaustive bibliography is included, from which the reader may obtain references to more detailed information on every subject covered.

* * * * *

Man cannot control travel into space until the difficult problems of atmospheric reentry have been solved. For many years to come, every manned vehicle leaving the earth's atmosphere will have to return to earth, either from a decaying satellite orbit or under the more direct influence of the earth's gravitational field. In either case, at some stage of its passage through the atmosphere, the vehicle will travel at very high velocities. This, in turn, will result in high deceleration and the release of large quantities of thermal energy. If

either man or sensitive equipment is to survive inside such a vehicle, both conditions will have to be controlled. Eventually, when more efficient propulsion methods have been developed, it may be possible to counter a space vehicle's kinetic energy by applying reverse thrust. That day is not yet in sight, however, and reentry remains a critical problem in space technology.

The difficulty of controlling reentry is well exemplified by the fact that almost all meteorites entering the earth's atmosphere are burned up before they reach the surface of the earth. The few that do reach the earth retain only a small proportion of their initial mass, and the temperature developed inside would probably have eliminated any life present at the time of reentry. Meteorites have random physical characteristics. Most of them enter the atmosphere at speeds well above escape or circular velocities, and in entering the atmosphere they follow random trajectories. This paper is intended to show how man-made vehicles can be designed and controlled in flight so as to survive atmospheric reentry and experience no disastrous effects.

* * * * *

The mathematical analysis of reentry dynamics and thermodynamics is tremendously complex. The equations of state needed to obtain useful results depend upon a great many constants and variables. In fact, it has been impossible thus far to arrive at exact general relationships that could be applied to specific cases. Instead we have had to simplify the problem by assuming such things as an invariable gravitational field, disregarding the effects of the rotation of the earth, and so on. (These simplifying assumptions will be explained as they arise in this paper.) It is believed that, despite the use of these assumptions, all the results are valid; many of them have already been experimentally verified.

The difficulties associated with reentry have long been known, especially by astronomers, who frequently saw streaks of light in the night sky as meteorites burned up. The problem of reentry did not present itself in a practical manner until man reached a state of technical development at which he could move a sizable object out of the atmosphere and then require it to return to the earth's surface--or to the surface of some other planet surrounded by an atmosphere. This point in the technology was reached shortly before World War II, when German scientists designing ballistic missiles recognized that, in order to achieve any appreciable range (over 250 nautical miles), the warhead would have to leave the atmosphere and then reenter at an unavoidably high velocity.

Since those days the reentry problem has been further complicated by technical advances that now place mankind on the threshold of space travel, the successful development of long-range or intercontinental ballistic missiles (ICBMs) and other similar projects. Thus reentry is no longer a subject for theoretical investigation alone; in this active area, theory and empirical results are blending in attempts to find answers to some pressing practical questions. Various branches of science--celestial mechanics, thermodynamics, solid-state physics and gas dynamics--are involved in the search for solutions to the problems of atmospheric reentry.

2. FUNDAMENTAL PRINCIPLES

2.1 Celestial Mechanics.

For all practical purposes there are essentially three types of uncontrolled atmospheric penetration:

(1) Direct entry from outer space, which is often a relatively steep path of descent and at times almost a straight line

(2) The parabolic approach of a ballistic missile

(3) The gradually descending path characteristic of a decaying satellite orbit.

A number of factors affect the trajectory of a body moving above the surface of the earth, e.g., Coriolis force, lunar gravitation; but most of them can be disregarded in the study of reentry physics because, at best, reentry analysis can furnish only approximate values for such variables as total heat transfer. Disregarding certain variations in the trajectory is not likely to cause more of an error in the final results than failing to consider such unpredictable variations as wind velocity during reentry, moisture content and anomalies in air density.

In the first type of atmospheric penetration (direct entry from outer space) the vehicle would have to approach at a steep angle to ensure that it enters the earth's gravitational field and lands in a single pass. (A requirement for single-pass landing is assumed through this paper, unless otherwise indicated.) The vehicle's velocity for an entry from outer space would be at least as high as its escape velocity (37,000 feet per second), or about 26,000 feet per second in the case of a decaying satellite circular orbit (ref. 209).

In its parabolic flight, a ballistic missile fails to leave the earth's gravitational field and does not complete an orbit around the earth.

A satellite can reenter the atmosphere via several possible approaches: (1) a great-circle flight at small angles of inclination, (2) a great-circle flight at large angles of inclination, (3) a minor-circle flight at small angles of inclination and (4) a minor-circle flight at large angles of inclination. The first and third possibilities are

typical of circular orbits, while the second and fourth represent elliptical orbits.

2.2 Analysis of a Space Vehicle's Energy.

A body approaching the atmosphere of a planet possesses a great amount of energy--kinetic energy generated by the body's motion and potential energy created by the gravitational force of the planet. Usually there is greater kinetic than potential energy. For example, a vehicle approaching the earth from outer space at escape velocity would have about 26,000 Btu per pound of kinetic energy. All the kinetic and potential--or total--energy of the reentry body must be converted into some other form by the time the body comes to rest.

The vehicle's kinetic energy at the time of reentry is $\frac{1}{2} m v^2$. The potential energy is equal to mgy, where y represents the altitude of reentry. (The reentry altitude in this paper will be taken as 3×10^5 feet unless otherwise indicated.) Therefore,

$$E = \frac{1}{2} m v^2 + 3 \times 10^5 m g$$

and since g can be taken as approximately 32.2 fps^2 on the basis of the simplifying assumption that $\frac{R_o}{R_o + y} \simeq 1$.

The total energy of the vehicle at the instant of reentry is approximately

$$E = \frac{1}{2} m v^2 + 10^7 m = m\left(\frac{1}{2} v^2 + 10^7\right)$$

2.3 The Earth's Atmosphere.

In the solution of reentry problems, a very important factor is the earth's atmosphere, particularly its characteristics at various altitudes. Our atmosphere is a mixture of various gases. At lower altitudes (up to about 30 kilometers from the earth's surface), these gases consist mainly of diatomic oxygen and nitrogen. At greater heights we find significant concentrations of other nuclear configurations. At 30 kilometers a significant concentration of ozone (O_3) builds up, and, still further, oxygen and nitrogen tend to dissociate into single atomic particles no longer in nuclear structure. At still higher altitudes, there is a significant concentration of ionized hydrogen. Figure 1 is a detailed breakdown of the earth's atmosphere up to an altitude of 33 kilometers.

The density distribution of the atmosphere also varies with altitude. The latest study available on this subject (ref. 1) indicates

Gas	10^6 x fraction (volume)	Amount (C_M, S. P. T.)
N_2	780, 900	624, 600
O_2	209, 500	167, 600
A	9, 300	7, 440
CO_2	300	220
Ne	18	14
He	5. 2	4. 2
CH_4	1. 5	1. 2
Kr	1	0. 8
N_2O	0. 5	0. 4
H_2	0. 5	0. 4
O_3	0. 4	0. 3
Xe	0. 08	0.06
H_2O	10^3-10^4	10^3-10^4

Figure 1. Composition of dry atmosphere
(Taken from reference 223.)

FIGURE 2

ATMOSPHERE'S DENSITY-DISTRIBUTION CURVE, BASED ON SATELLITE EXPERIMENTS

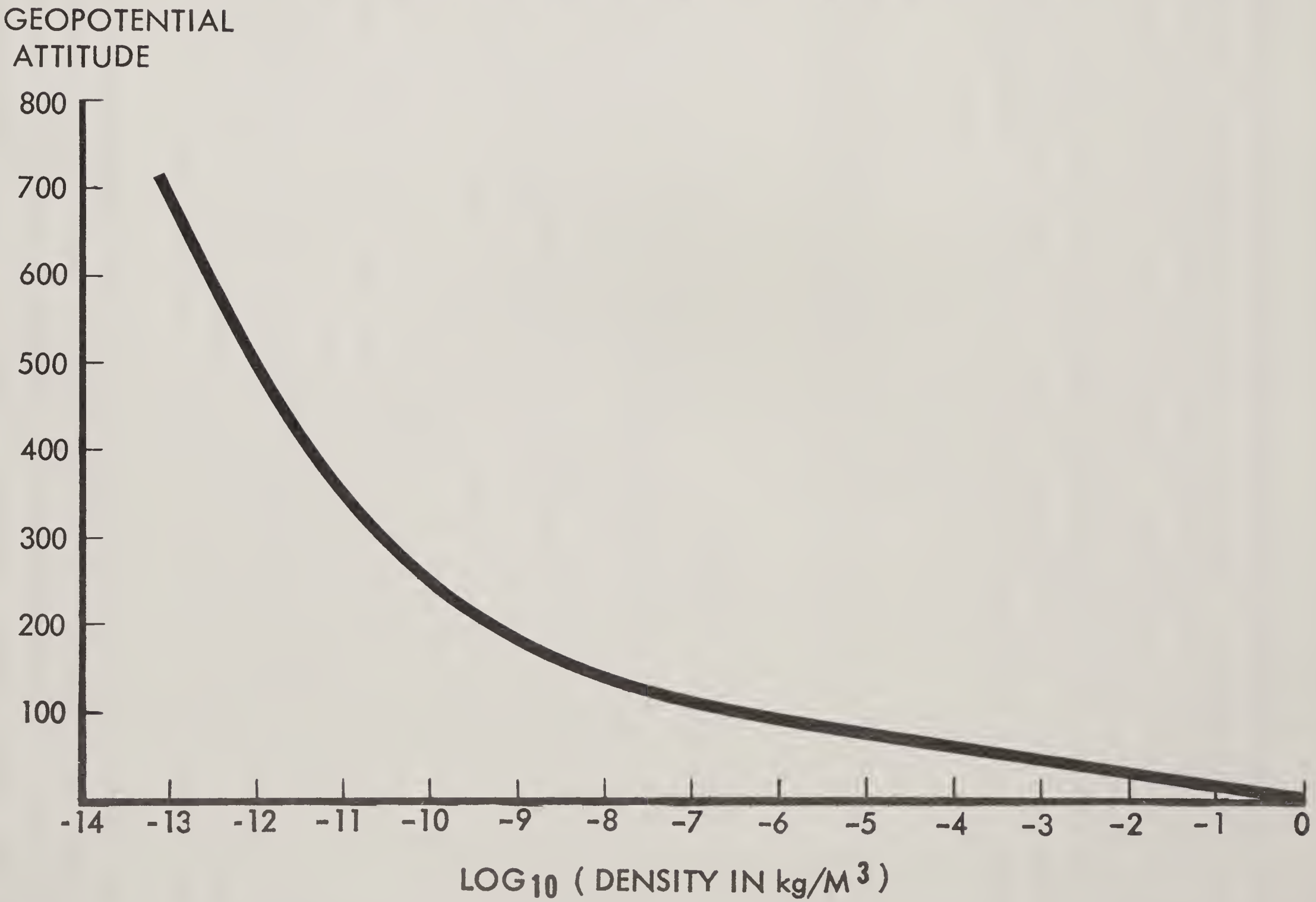

that the density is considerably greater at higher altitudes than was previously believed (that is, before 1956). The most recent density-distribution curve based on satellite experiments is shown in Figure 2.

The temperature of the atmosphere is also an important factor in reentry problems. Although it varies considerably with altitude, the temperature has an average value of 240°K, and this is frequently used in reentry calculations. Employing the average temperature, it is possible to obtain the "atmospheric parameter," β, or the reciprocal characteristic height of the atmosphere. For earth, this factor is taken as $\beta^{-1} = 23,500$ feet. Then, by integrating the hydrostatic equation, it is possible to obtain the distribution of density with altitude,

$$\frac{\rho_y}{\rho_o} = e^{-y\beta}$$

where ρ_o is a reference density, sometimes assumed equal to ρ_{SL} (ref. 1, 215).

2.4 Dynamics of Reentry.

2.4.1 General Equations of Motion: The determination of deceleration heating rates and other critical values associated with reentry are based to a large degree on the fundamental equations of motion. It is therefore particularly important to obtain a clear understanding of reentry dynamics. The purpose of this section is to develop the general equations of motion; their application to specific reentry problems will be treated in section 2.4.2.

The general differential equations describing the motion of a reentry body cannot be solved in the usual manner. It is necessary to make certain simplifying assumptions, such as disregarding the effect of certain variables or assuming that they remain constant during considerable periods of time. These assumptions can be made when considering specific reentry problems without serious inaccuracies.

There are several approaches for developing the equations of motion, all of them based on Newtonian dynamics. For the purposes of this paper, two methods of developing the general equations of motion will be demonstrated. Using the principle of conservation of momentum, we have

$$-\frac{dv}{dt} = -g \sin\theta + \frac{\rho v^2}{2m}(C_D A)$$

$$\frac{v}{\cos\theta}\frac{d\theta}{dt} = g - \frac{v^2}{r} - \frac{\rho v^2}{2m\cos\theta}(C_L A)$$

The first equation represents the momentum balance in the direction of motion, and the second equation, the momentum of balance normal to the direction of motion (ref. 215).

A vectorial approach to the fundamental equations of motion yields the following:

$$\vec{a} = \left(\frac{dv_2}{dt} - \frac{v_1^2}{r}\right) i_r + \left(\frac{dv_1}{dt} + \frac{v_1 v_2}{r}\right) i_\theta$$

If θ is the local flight path angle, we have $\theta = \frac{v_2}{v_1}$ and the aerodynamic force is

$$F = \left(-mg + L\cos\theta - D\sin\theta\right) i_r - \left(D\cos\theta + L\sin\theta\right) i_\theta$$

and in Newtonian mechanics, where force equals mass multiplied by acceleration, we have

$$-mg + L\cos\theta - D\sin\theta = m\left(\frac{dv_2}{dt} - \frac{v_1^2}{r}\right)$$

$$\frac{dv_2}{dt} = -g + \frac{L}{m}\cos\theta - \frac{D}{m}\sin\theta + \frac{v_1^2}{r} \quad \text{and}$$

$$-D\cos\theta - L\sin\theta = m\left(\frac{dv_1}{dt} + \frac{v_1 v_2}{r}\right) \tag{1}$$

$$\frac{dv_1}{dt} + \frac{v_1 v_2}{r} = -\frac{D}{m}\cos\theta - \frac{L}{m}\sin\theta \tag{2}$$

The first set of equations above represents the fundamental equations of motion in terms of the absolute instantaneous velocity (v), and the second set are in terms of the vertical (v_2) and horizontal (v_1) velocity components.

2.4.2 Solution of the Equations of Motion: To solve the equations of motion developed in section 2.4.1, certain simplifying assumptions must be made. They should, in general, have no serious effect on the calculated deceleration and convective aerodynamic heating rates, where they reach dominant values. Six general assumptions of this

nature can be made, while others depend on specific reentry conditions such as the body's shape, the trajectory, the magnitude of the lift coefficient, etc. The six general assumptions are as follows:

(1) Both the atmosphere and earth are perfect spheres.

(2) $$\frac{d\bar{T}_\omega}{\bar{T}_\omega} \ll \frac{d\rho_\omega}{\rho_\omega}$$

(3) $$\frac{d\bar{M}}{\bar{M}} \ll \frac{d\rho_\omega}{\rho_\omega}$$

(4) $$\frac{dr}{r} \ll \frac{dv_1}{v_1}$$

(5) The peripheral velocity of the earth or its atmosphere is negligibly small compared to the velocity of reentry.

(6) There are two possibilities of reentry: (a) without a lift force (or L = 0) and (b) with a lift force, but usually at a very small angle of reentry so that the horizontal component of lift is small compared to the drag. This is equivalent to saying that

$$\left|\frac{L}{D}\tan\theta\right| \ll 1$$

We now take equations of motion (1) and (2) developed in the section 2.4.1:

$$-D\cos\theta - L\sin\theta = m\left(\frac{dv_1}{dt} + \frac{v_1 v_2}{r}\right) \qquad (1)$$

$$\frac{dv_1}{dt} + \frac{v_1 v_2}{r} = -\frac{D}{m}\cos\theta - \frac{L}{m}\sin\theta \qquad (2)$$

From the fourth assumption we have

$$\frac{\frac{dr}{r}}{\frac{dv_1}{v_1}} \ll 1$$

But

$$\frac{\frac{dr}{r}}{\frac{dv_1}{v_1}} = \frac{v_1\left(\frac{dr}{dt}\right)}{r\left(\frac{dv_1}{dt}\right)} = \frac{\frac{v_1 v_2}{r}}{\frac{dv_1}{dt}} \qquad \therefore \frac{\frac{v_1 v_2}{r}}{\frac{dv_1}{dt}} \ll 1 \qquad (3)$$

In the second equation of motion, $\therefore \frac{v_1 v_2}{r}$ **can be neglected, and we have**

$$\frac{dv_1}{dt} = -\frac{D}{m}\cos\theta\left(1+\frac{L}{D}\tan\theta\right). \qquad (4)$$

But we have seen that as a result of the sixth assumption either

$$\frac{L}{D}\tan\theta = 0 \qquad \text{or} \qquad \left|\frac{L}{D}\tan\theta\right| \ll 1$$

In any event it can be disregarded, and we have

$$\frac{dv_1}{dt} = \left[\frac{\rho_\infty}{2\left(\frac{m}{C_D A}\right)}\right]\left[\frac{v_1}{\cos\theta}\right] \qquad (5)$$

which is based on the relationship for drag:

$$D = \frac{1}{2}\rho_\infty v^2 A C_D \quad \text{where} \quad v = \sqrt{v_1^2 + v_2^2}\,.$$

At this point we make use of a new, dimensionless variable:

$$\bar{v} = \frac{v_1}{v_c} \quad \text{or} \quad \bar{v} = \frac{v_1}{\sqrt{gr}}$$

Also from the law of gravitation:

$$\frac{dg}{g} = -2\frac{dr}{r}$$

and from the fourth assumption we can disregard the derivatives of g with respect to those of v_1 **, and since** $v_1 = \bar{v}\sqrt{gr}$ **we have**

$$\frac{dv_1}{dt} = \sqrt{gr}\,\frac{d\bar{v}}{dt} \qquad \frac{dv_2}{dt} = \frac{d^2y}{dt^2} \qquad (6)$$

Applying this to the first equation of motion, together with the drag coefficient,

$$-\frac{1}{g}\frac{dv_2}{dt} = -\frac{1}{g}\frac{d^2y}{dt^2} = 1 - \bar{v}^2 + \frac{\rho_\infty}{2}\frac{C_D A \pi \bar{v}^2}{m\cos^2\theta}\left(\sin\theta - \frac{L}{D}\cos\theta\right) \tag{7}$$

In order to reduce these two equations of motions into a single equation, a new dimensionless, dependent variable, Z, is introduced as follows:

$$Z = \frac{\rho_\infty}{2\left(\frac{m}{C_D A}\right)}\sqrt{\frac{\pi}{\beta}}\ \bar{v} \tag{8}$$

where $\bar{v}$ is the independent variable, and $Z' = \frac{dZ}{d\bar{v}}$.

Using the well-known local-density/altitude-variation equation,

$$-\frac{1}{\rho_\infty}\frac{d\rho_\infty}{dy} = \beta$$

we can easily develop the following relationship, which is dependent on the fourth assumption:

$$\frac{Z'}{\bar{v}} - \frac{Z}{\bar{v}^2} = -\frac{\rho_\infty\sqrt{\pi\beta}}{2\left(\frac{m}{C_D A}\right)}\frac{dy}{d\bar{v}} \tag{9}$$

$$\therefore\quad \frac{Z'}{\bar{v}} - \frac{Z}{\bar{v}^2} = -\beta\frac{Z}{\bar{v}}\frac{dy}{dt}\frac{dt}{d\bar{v}} \tag{10}$$

Then $$\frac{d\bar{v}}{dt} = -\sqrt{g\beta}\ \frac{\bar{v}Z}{\cos\theta}\ . \tag{11}$$

Substituting in equation (10) and noting that $\frac{dy}{dt} = v_2$

and $v_2 = \bar{v}\sqrt{g\pi}\ \tan\theta$ we have

$$Z' - \frac{Z}{\bar{v}} = \sqrt{\frac{\beta}{g}}\ \frac{\cos\theta}{\bar{v}}\ \frac{dy}{dt} \tag{12}$$

and $$Z' - \frac{Z}{\bar{v}} = \sqrt{\beta\pi}\ \sin\theta \tag{13}$$

Differentiating with respect to v_2 and $\sin\theta$ in equation (12) the results are

$$\frac{1}{g}\frac{dv_2}{dt} = \sqrt{\frac{\pi}{g}}\ \frac{d}{dt}\left(\frac{\bar{v}\sin\theta}{\cos\theta}\right) \tag{14}$$

and

$$\frac{1}{g}\frac{dv_2}{dt} = \frac{1}{\sqrt{\beta g}}\frac{d\bar{v}}{dt}\left(\frac{\bar{v}Z''}{\cos\theta} + \frac{\bar{v}\sqrt{\beta\pi}\sin^2\theta}{\cos^2\theta}\frac{d\theta}{d\bar{v}}\right). \tag{15}$$

The term $\frac{d\theta}{d\bar{v}}$ represents the flight-path curvature. Also from equation (12) we have:

$$\bar{v}\frac{d}{d\bar{v}}\left(Z' - \frac{Z}{\bar{v}}\right) = \bar{v}\sqrt{\beta\pi}\ \frac{d\sin\theta}{d\bar{v}}. \tag{16}$$

Substituting (16) and (11) into (15), the result is

$$-\frac{1}{g}\frac{d^2y}{dt^2} = \frac{\bar{v}Z}{\cos^2\theta}\left\{\bar{v}Z'' + \tan^2\theta\left[\bar{v}\frac{d}{d\bar{v}}\left(Z' - \frac{Z}{\bar{v}}\right)\right]\right\}. \tag{17}$$

From the definition of the Z function and equation (12), we note that equation (7) can be presented as

(18)

$$-\frac{1}{g}\frac{dv_2}{dt} = -\frac{1}{g}\frac{d^2y}{dt^2} = 1 - \bar{v}^2 + \frac{\bar{v}Z}{\cos^2\theta}\left(Z' - \frac{Z}{\bar{v}} - \sqrt{\beta\pi}\,\frac{L}{D}\cos\theta\right).$$

Comparing equation (18) with equation (17) and noting that

$$\bar{v}\frac{d}{d\bar{v}}\left(Z' - \frac{Z}{\bar{v}}\right) = \bar{v}Z'' - Z' + \frac{Z}{\bar{v}}$$

or that

$$Z' - \frac{Z}{\bar{v}} = \bar{v}Z'' - \bar{v}\frac{d}{d\bar{v}}\left(Z' - \frac{Z}{\bar{v}}\right)$$

we can develop the relationship

$$\bar{v} Z'' - Z' + \frac{Z}{\bar{v}} = \frac{1 - \bar{v}^2}{\bar{v} Z} \cos^4\theta - \sqrt{\beta\pi}\,\frac{L}{D}\cos^3\theta \tag{19}$$

and

$$\bar{v}\,\frac{d}{d\bar{v}}\left(\frac{dZ}{d\bar{v}} - \frac{Z}{\bar{v}}\right) - \frac{1-\bar{v}^2}{\bar{v} Z}\cos^4\theta + \sqrt{\beta\pi}\,\frac{L}{D}\cos^3\theta = 0. \tag{20}$$

It is therefore obvious that the two fundamental equations of motion have been reduced to a single second-order differential equation involving the Z function as a dependent variable and the $\bar{v}$ function as the independent variable. Further, it should be noted that equation (20) is nonlinear owing to the term $\frac{1-\bar{v}^2}{\bar{v} Z}\cos^4\theta$ which represents the effects of gravitation and centrifugal forces.

Computer methods can be used to calculate the Z function in equation (20); also, numerical methods can be used to compute the Z function stepwise from this nonlinear equation. Direct integration methods, however, have not yet been developed. One method, probably not very accurate, is simple because it involves the repetition of many identical operations. Suppose we have an initial value of $\bar{v} = \bar{v}_n$ and the corresponding value of $Z = Z_n$ and $Z' = Z'_n$. Setting $\cos\theta = 1$ for simplicity, we have for the second derivative

$$Z_n'' = \frac{1}{\bar{v}_n}\left(Z_n' - \frac{Z_n'}{\bar{v}_n} + \frac{1-\bar{v}_n^2}{\bar{v}_n Z_n} - \sqrt{\beta\pi}\,\frac{L}{D}\right) \tag{21}$$

and for the third derivative

$$Z_n''' = \frac{1}{\bar{v}_n}\left[\frac{1}{\bar{v}_n}\left(Z' - \frac{Z_n}{\bar{v}_n}\right) - \frac{1-\bar{v}_n^2}{\bar{v}_n}\,\frac{Z_n'}{Z_n^2} - \frac{1+\bar{v}_n^2}{\bar{v}_n^2 Z_n}\right]. \tag{22}$$

Using the Taylor expansion for Z_{n+1} and Z'_{n+1} at the next point $\bar{v}_{n+1}$, we have

$$Z_{n+1} = Z_n + Z_n'\,\Delta\bar{v} + Z_n''\,\frac{\Delta\bar{v}^2}{2} + Z_n'''\,\frac{\Delta\bar{v}^3}{6} + \cdots\cdots$$

$$Z'_{n+1} = Z_n' + Z_n''\,\Delta\bar{v} + Z_n'''\,\frac{\Delta\bar{v}}{2} + \cdots\cdots$$

and for $\Delta\bar{v}$ a fairly small value has to be selected e.g., between 0.001 and 0.002.

A large number of Z functions have been calculated for atmospheric reentry on a computer (ref. 48).

As a result of the methods used for its derivation, it is clear that the single equation of motion (20) will be applicable to ballistic (nonlifting) vehicles irrespective of the flight path angle at reentry, while in the case of lifting vehicles

$$\left| \frac{L}{D} \tan \theta \right| \ll 1.$$

This last inequality implies that, for lifting vehicles, either the lift coefficient must be very small indeed or the reentry angle must be quite small.

2.4.3 Effect of Reentry Trajectory: As we have already seen, there are many factors that influence the rate of heat absorption and deceleration of a vehicle entering the earth's atmosphere. One factor is the trajectory of entry, which will affect the vehicle designed to provide some aerodynamic lift as well as the nonlifting variety (a ballistic capsule).

First let us consider the case of a nonlifting vehicle. For practical purposes it may be assumed that all vehicles enter the atmosphere at about the same (escape) velocity, 26,000 fps. Two factors with respect to the entering vehicle that will strongly influence heat-absorption rates and peak deceleration values are the entry angle θ_E and the value of $\frac{C_D A}{W}$ for the particular vehicle under consideration. The entry angle is the minimum angle between the line of flight and any line in the tangential plane to the atmosphere at the point of entry. The point-of-entry altitude is usually taken to be about 300,000 to 400,000 feet.

Disregarding the value of $\frac{C_D A}{W}$ for the moment, it has been found (ref. 193) that peak deceleration is proportional to the entry angle. The lowest peak deceleration occurs in the case of a "grazing" entry resulting from a decaying satellite orbit, that is, $\theta_E = 0$. In this instance the peak deceleration amounts to about 9 g. The altitude at which this deceleration occurs, however, is controlled by the value of $\frac{C_D A}{W}$; the lower this value, the higher the altitude of maximum deceleration (as will be shown later). With increasing θ_E the value of peak deceleration increases, at first slowly, but later more abruptly, as shown in Figure 3. It may be assumed that for some time space vehicles will not be large enough to provide any type of effective deceleration counteraction for its occupants. Consequently the maximum

FIGURE 3

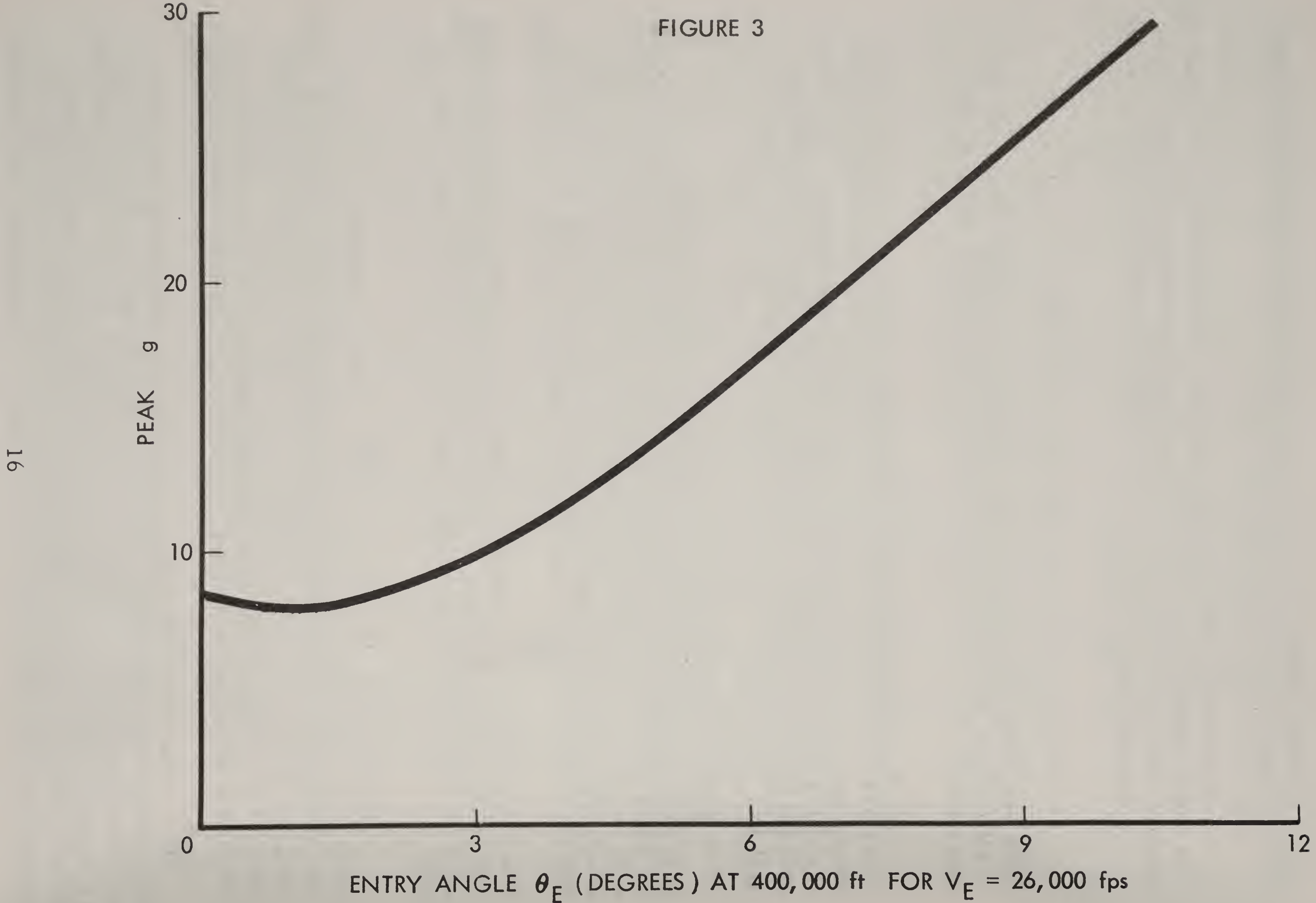
30
20
10
0
3
6
9
12
PEAK g
16
ENTRY ANGLE θ_E (DEGREES) AT 400,000 ft FOR V_E = 26,000 fps

deceleration value will probably not be allowed to exceed about 10 g, since this is probably the maximum deceleration rate a trained pilot can withstand without ill effects physiologically. (This value was suggested by Dr. Halvey, ref. 219.)

As indicated on Figure 3, this value is reached at about $\theta_E = 3°$ for a vehicle entering at about 26,000 fps.

As indicated before, the altitude at which peak deceleration occurs depends on the value of $\frac{C_D A}{W}$. For a higher value of this variable, the maximum deceleration will occur at a higher altitude. The actual magnitude of the peak deceleration, however, is not significantly affected--merely the altitude at which it occurs. Figure 4 shows the variation of vehicle velocity with altitude for three widely diverging values of $\frac{C_D A}{W}$. The curves were developed by K. A. Ehricke and R. Hermann (ref. 208, 219). Figure 4 clearly shows that, for a given altitude, the velocity of a vehicle with a high $\frac{C_D A}{W}$ value is much higher than that of one with a low value, all other variables being equal --such as reentry velocity (assumed to be circular velocity, about 26,000 fps) and entry angle. This confirms the conclusion previously stated that peak deceleration for vehicles having low $\frac{C_D A}{W}$ occurs at much lower altitudes or that the deceleration rate for such vehicles in the the upper regions of the atmosphere is very low.

Another useful set of curves is shown in Figure 5. Here is a curve for each of a set of reentering vehicles with varying values of $\frac{C_D A}{W}$, where the altitude is plotted vs. the dimensionless $\frac{a}{g}$ ratio. Again we see that, for low $\frac{C_D A}{W}$ values, peak deceleration occurs at lower altitudes.

Next we have to consider reentry vehicles that have some lifting capacity, in other words, $C_L > 0$. Vehicles in this class are limited by three considerations in particular: The first is the boundary imposed by maximum deceleration; again we are limited by a maximum of 10 g. A set of curves for various values of $\frac{C_L}{C_D}$ is shown in Figure 6, in which peak g is plotted vs. the entry angle. Second, the vehicle is limited by the maximum skin temperature of the airfoil, or lifting surface. Usually taken as 2500°R, this temperature is measured one foot from the leading edge of the airfoil, based on the equilibrium between convective heat transfer to the airfoil and the radiative heat

FIGURE 4

VARIATION OF VEHICLE VELOCITY WITH ALTITUDE

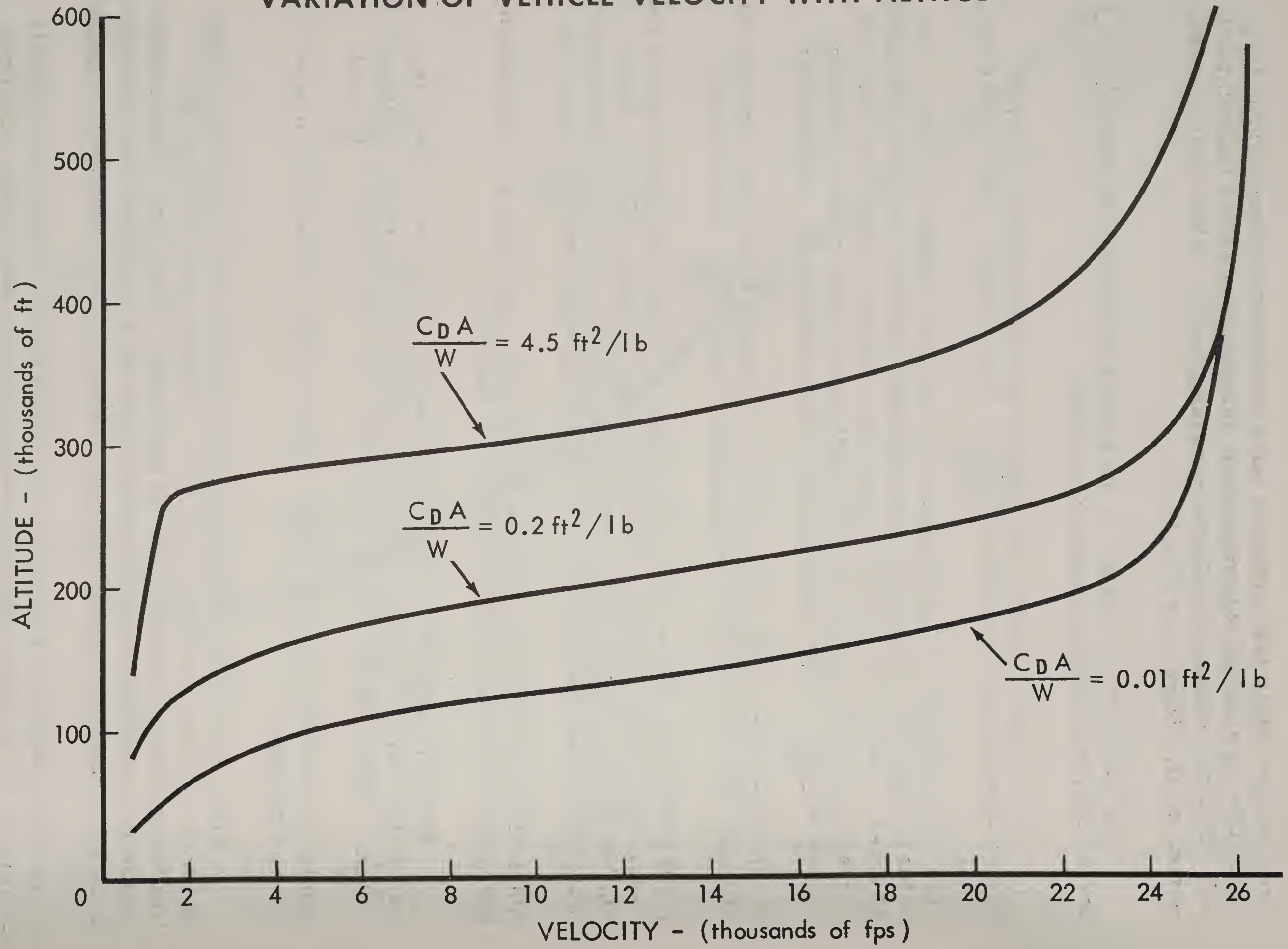

FIGURE 5

ALTITUDE vs. DIMENSIONLESS $\frac{a}{g}$ RATIO

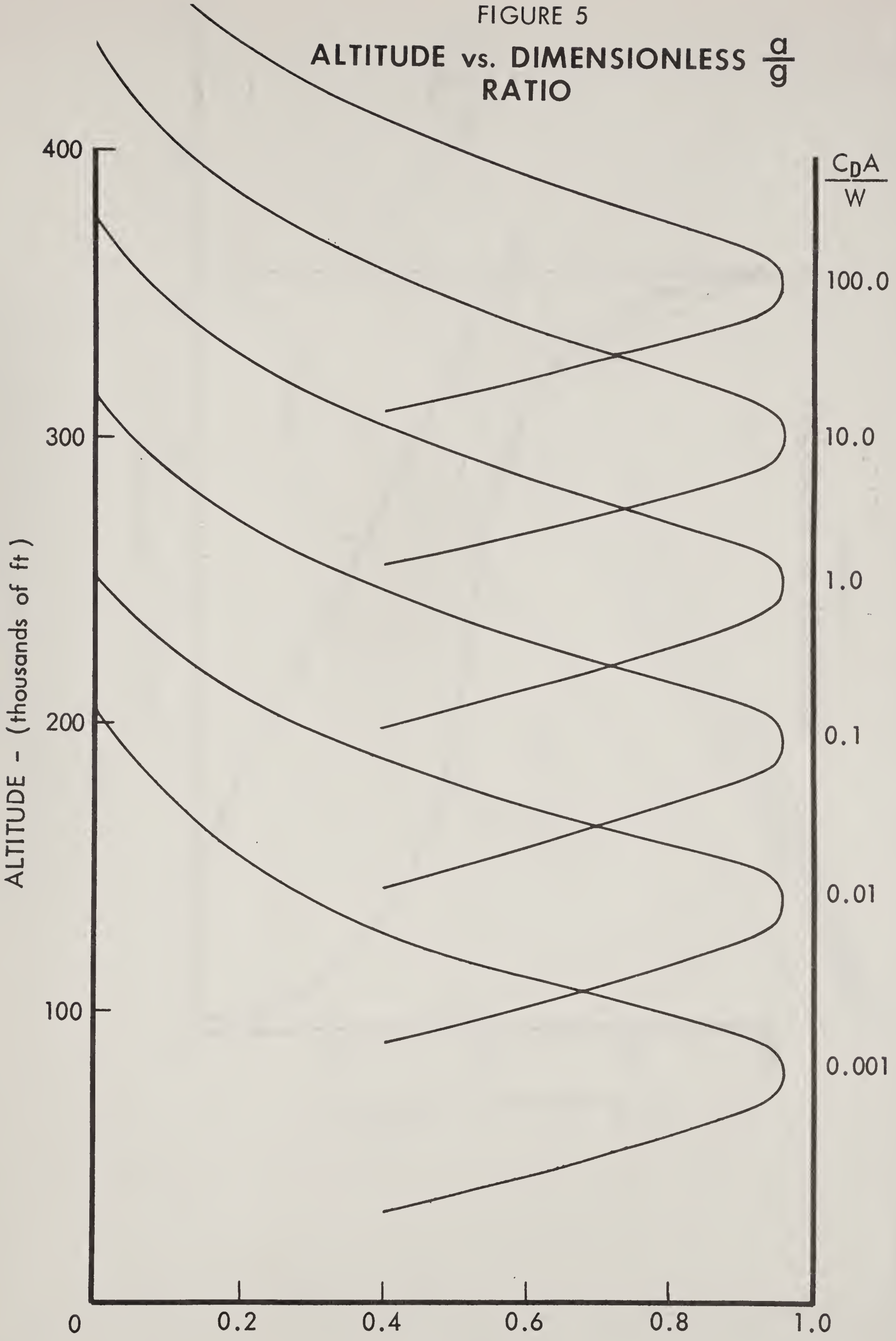

FIGURE 7

ALTITUDE vs. VELOCITY

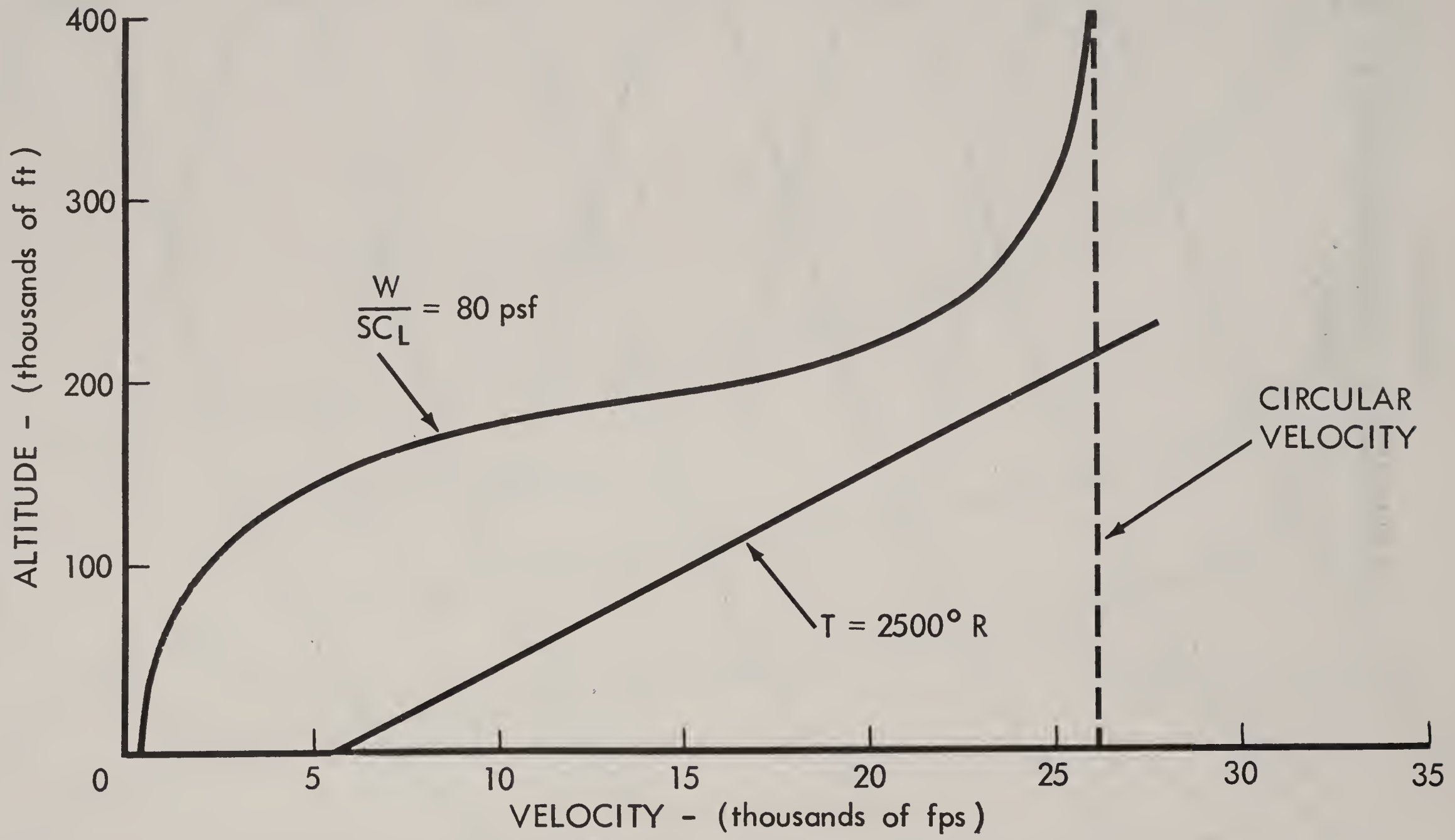

FIGURE 6

PEAK g vs. ENTRY ANGLE

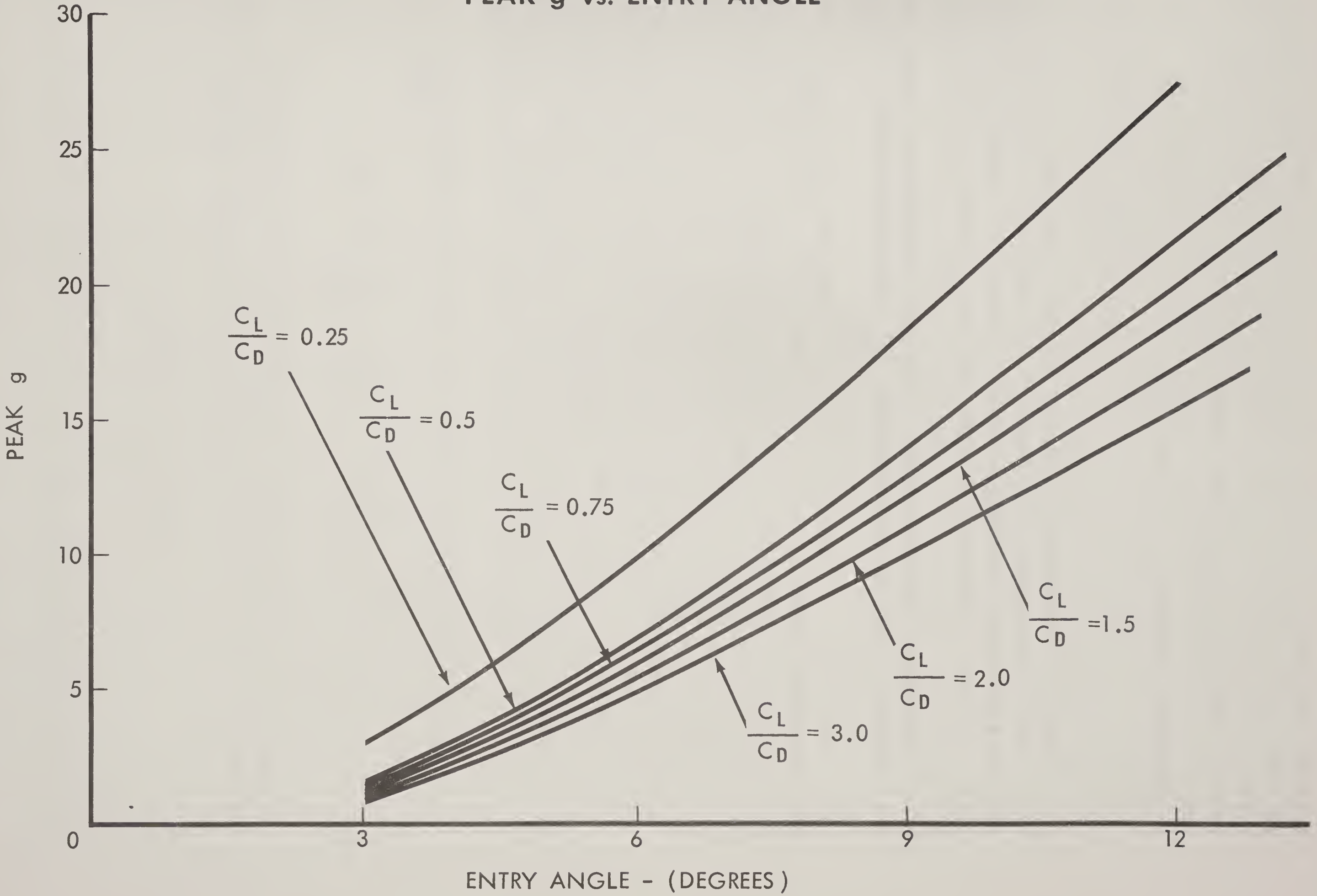

transfer away from the airfoil. This state is referred to as radiation equilibrium temperature. The third boundary is imposed by the minimum aerodynamic lift required to overcome the apparent weight of the vehicle, that is, the difference between the real weight caused by gravitational attraction and the action of the centrifugal forces. The mathematical relationship is obviously

$$W - \frac{W v^2}{g r} = S C_L q.$$

Figure 7 shows the boundaries imposed by the last two restrictions, that is, maximum permissible skin temperature and minimum velocity for balancing the apparent weight of a vehicle having a value $\frac{W}{S C_L}$ = 80 psf. From Figure 6 we can conclude that the entry angle for acceptable peak deceleration (<10 g) can vary between 6° and 9° for a lifting vehicle (with a maximum $\frac{C_L}{C_D}$ from 0.25 to 3.0). This figure compares very favorably with the maximum entry angle of 3° for a nonlifting vehicle.

3. AERODYNAMIC HEATING

The heat that is produced around a space vehicle and is then transferred to the vehicle's surface is one of the two most serious problems encountered during reentry. Several techniques of coping with the large quantity of heat produced have been developed (see section 5). However, in order to determine the most suitable method for cooling the surface of a particular reentry vehicle and to ensure that the amount of coolant is neither insufficient for the task nor so excessive as to result in a waste of payload capacity, it is necessary to predict theoretically the total amount of heat likely to be absorbed and the peak heating rate that may be encountered. Consequently it is of great importance to develop mathematical solutions for these problems.

The purpose of this section is to present useful analytical methods of providing approximate values for aerodynamic heating created during reentry, without regard for vehicle configuration or trajectory during descent. The objective, therefore, is to develop very general relationships between variables that affect aerodynamic heating so that they can be applied to specific cases. Also, it is possible to obtain mathematical relationships that are only suitable for limited designs and trajectories, as will be indicated later in one or two instances. Although more precise, mathematical relationships are usually of less value in efforts to select--and even improve on--designs for specific missions. The following mathematics is largely based on the general equations of motion and their solution (see section 2).

The stagnation heating rate can be represented as follows (ref. 224):

$$q_s = \frac{C}{\sqrt{R}} \left(\frac{\rho_\infty}{\rho_{SL}} \right)^n \left(\frac{\bar{V}}{\cos \theta} \right)^m \tag{23}$$

In equation (23) the constants C, n and m depend on the type of boundary layer flow. These constants, calculated in various papers (e.g., ref 241), have been found to be:

$$16,800 < C < 19,800$$
$$3.1 < m < 3.22$$

We can take for laminar flow $n = \frac{1}{2}$. For simplicity, m can be taken as equal to 3 and C as equal to 17,000 Btu $ft^{-\frac{3}{2}}$ sec^{-1}. The value

for C is based on the mean results obtained thus far for air at near-peak heating velocities, that is, $\bar{v} \simeq 0.8$

To develop useful equations for heat, it is necessary to relate the factor $\left(\frac{\rho_\infty}{\rho_{SL}}\right)$ in equation (23) to the Z function. This can be done as follows: It was seen from equation (8) that

$$Z = \frac{\rho_\infty}{2\left(\frac{m}{C_D A}\right)} \sqrt{\frac{\pi}{\beta}}\ \bar{v} \tag{24}$$

Therefore,

$$\frac{\rho_\infty}{\rho_{SL}} = \frac{2}{\rho_{SL}} \sqrt{\frac{\beta}{\pi}} \left(\frac{m}{C_D A}\right) \frac{Z}{\bar{v}} \tag{25}$$

Replacing this value in equation (23), we have

$$q_s = \frac{C}{\sqrt{R}} \left[\frac{2}{\rho_{SL}} \sqrt{\frac{\beta}{\pi}} \frac{m}{C_D A} \left(\frac{Z}{\bar{v}} \right) \right]^{\frac{1}{2}} \left[\frac{\bar{v}}{\cos\theta} \right]^3$$

$$q_s = 2C R^{-\frac{1}{2}} \rho_{SL}^{-\frac{1}{2}} \beta^{\frac{1}{4}} \pi^{-\frac{1}{4}} m^{\frac{1}{2}} C_D^{-\frac{1}{2}} A^{-\frac{1}{2}} Z^{\frac{1}{2}} \bar{v}^{\frac{5}{2}} \cos^{-3}\theta . \tag{26}$$

If $k_1 = \frac{q_1}{q_s}$, and inserting the various values for C, ρ_{SL}, etc., equation (26) is reduced to

$$q_1 = 590 \left(k_1 \sqrt{\frac{m}{C_D A R}} \right) \frac{\bar{v}^{\frac{5}{2}} Z^{\frac{1}{2}}}{\cos^3\theta} \tag{27}$$

The foregoing equation is based on the assumption of laminar flow. In the event of turbulence, the powers of $\bar{v}$ and Z must be changed to 2.2 and 0.8, respectively.

An analysis of equation (27) indicated that the factor

$$\left(k_1 \sqrt{\frac{m}{C_D A R}} \right)$$

represents the influence on the heat flux by the configuration of the vehicle while the factor $\frac{\bar{v}^{\frac{5}{2}} Z^{\frac{1}{2}}}{\cos^3\theta}$ is the effect of the trajectory as determined by the lift/drag ratio.

Equation (27), of course, is particularly useful in studying the effect of heat for vehicles which are cooled by reflectance (see section

5). For vehicles that use cooling system of the heat-sink variety, it is much more important to know the total heat absorbed during reentry. This can be determined as follows:

$$Q = \int\int q_1 \, dt \, ds. \tag{28}$$

Now going back to section 2.4.1 we have from equation (11)

$$\frac{d\bar{v}}{dt} = -\sqrt{g\beta}\,\frac{\bar{v} Z}{\cos\theta} \tag{29}$$

$$dt = -\frac{\cos\theta}{\bar{v} Z \sqrt{g\beta}}\, d\bar{v} \tag{30}$$

and integrating

$$t = -\int_{\bar{v}_1}^{\bar{v}_2} \frac{\cos\theta}{\bar{v} Z \sqrt{g\beta}}\, d\bar{v} \quad \text{or} \quad t = \frac{1}{\sqrt{g\beta}} \int_{\bar{v}_2}^{\bar{v}_1} \frac{\cos\theta}{\bar{v} Z \sqrt{g\beta}}\, d\bar{v}. \tag{31}$$

Combining the relationships in equations (27), (28) and (31), we have the following:

$$Q = 15,900 \sqrt{\frac{m}{C_D A R}} \int \frac{q_1}{q_s} ds \int_{\bar{v}_2}^{\bar{v}_1} \frac{\bar{v}^3}{Z^{\frac{1}{2}} \cos^2\theta} d\bar{v}. \tag{32}$$

One particularly important result of the preceding analysis is to determine the effect of a changing vehicle shape on the convective aerodynamic heating rate. From the Reynolds number, which has been calculated for many reentry vehicles, it has been established that air flow at near-peak heating ($\bar{v} \simeq 0.8$) is in the laminar, continuum-gas regime. Further, it was shown in equation (27) that for laminar flow the heating rate (q_1) is proportional to

$$\sqrt{\frac{m}{C_D A}} \left(\bar{v}^{\frac{5}{2}} Z^{\frac{1}{2}} \right).$$

Both C_D and Z tend to vary as the shape of the reentry vehicle changes. The dimensionless variable $\left(\bar{v}^{\frac{5}{2}} Z^{\frac{1}{2}} \right)$ is obviously an important factor tending to influence the heating rate. The maximum values

of this factor are shown in the following table as they vary with changing lift/drag ratio:

L/D	$\left(\bar{U}^{\frac{5}{2}} Z^{\frac{1}{2}}\right)_{MAX}$
-0.5	0.375
-0.25	0.302
-0.1	0.253
0	0.218
0.1	0.184
0.25	0.138
0.5	0.098
1.0	0.070

The values for $\left(\bar{U}^{\frac{5}{2}} Z^{\frac{1}{2}}\right)$ were obtained by solving for Z from equation (19) in section 2.4.2, disregarding vertical acceleration, vertical component of drag and by assuming that $\cos\theta \simeq 1$. These assumptions result in a simplified solution

$$Z = \frac{1 - \bar{U}^2}{\bar{U}\sqrt{\beta r}\left(\frac{L}{D}\right)}. \qquad (33)$$

This equation for Z is a reasonable approximation for a glide-reentry condition. The value of $\bar{U}$ for these calculations was taken as 0.8 when maximum heating occurs. The results shown in equation (33) are consistent with expectations, that is, the peak heating rate is inversely proportional to the lift force. In fact, if the drag force were a constant, the maximum heating rate would continue to decrease indefinitely with increasing lift. However, as the lift increases, so does the drag coefficient. Since

$$q_1 \sim \sqrt{\frac{m}{C_D A}}\left(\bar{U}^{\frac{5}{2}} Z^{\frac{1}{2}}\right) \qquad (34)$$

it is found that the heating rate drops continuously up to values of $\frac{L}{D} \simeq 0.75$. Beyond that there is a gradual increase in the heating rate for any particular shape.

The generalized heating theory is also usefully applied in determining how the drag coefficient value of a ballistic vehicle affects the

peak heating rate. First it is necessary to obtain an approximation for Z from equation (19). By disregarding the terms of gravity, centrifugal force and lift and assuming that the flight-path angle is constant, we have

$$Z = \sqrt{\beta r}\ (\sin\theta)\,\bar{v}\,\ln\frac{\bar{v}}{\bar{v}_i} \tag{35}$$

where $\bar{v}_i$ is some initial value of $\bar{v}$. Then from equation (27) for the ballistic case, we have

(36)

$$q_1 = 590\left[k_1\sqrt{\frac{m}{C_D A R}}\right]\left[\frac{\bar{v}^{\frac{5}{2}}}{\cos^3\theta}\right]\left[\sqrt{\beta r}(\sin\theta)\,\bar{v}\,\ln\frac{\bar{v}}{\bar{v}_i}\right]^{\frac{1}{2}}$$

Since θ is assumed to be constant for the ballistic design, it is clear that $q_{MAX} \sim \sqrt{\frac{m}{C_D A R}}$. The conclusion is that an increase in C_D, which is usually also accompanied by an increase in the radius of curvature of vehicle surface, causes a decrease in the maximum heating rate.

Although they will not be justified mathematically, two other important areas are associated with reentry heating: (1) the surface temperature of the vehicle under radiation equilibrium and (2) the effect of lift/drag ratio on the total heat absorbed.

It has been shown in several papers (ref. 216, 217, 221) that the maximum radiation-equilibrium temperature at laminar stagnation point tends to increase with increasing values of $\frac{m}{C_D A}$. At the same time, this temperature decreases as the value of L/D increases.

Thus, for high-lift vehicles, the temperature tends to remain lower than for ballistic designs of equal weight. It may be worthwhile to mention a number of values associated with radiation-equilibrium temperature that have been obtained from computers (ref. 219) using the relationship

$$\overline{T_{w_s}}\ \epsilon^{\frac{1}{4}} R^{\frac{1}{8}} = 3,840\left(\frac{W}{C_D A}\right)^{\frac{1}{8}}\left(\bar{v}^{\frac{5}{2}} Z^{\frac{1}{2}}\right). \tag{37}$$

For these calculations, L/D = 0.

$\frac{W}{C_D A}$	$(T_{w_s})_{MAX} R^{\frac{1}{8}} \epsilon^{\frac{1}{4}}$
0.3	2200
4	3100
10	3500
40	4100

It has just been shown that the peak heating rate can be frequently reduced by increasing the lift/drag ratio. Increased lift prevents the vehicle from descending as rapidly as it would otherwise, which has the adverse effect of increasing the time of exposure to heating. As may be expected from equation (28),

$$Q = \int\int q_1 \, dt \, dS$$

a reduction in heating rate (q_1), accompanied by a substantial increase in the upper limit of the first integral, could easily cause an increase in the total amount of heat taken in by the reentry vehicle. That is, in fact, what happens, as may be seen from the equation developed by Allen and Eggers (ref. 21):

$$Q = \frac{C_F}{C_D}\left(\frac{S}{A}\right)\left(\frac{1}{2} m v^2\right) \qquad (38)$$

Here a net increase in L/D gives rise to an increase in the effective laminar skin-friction coefficient (C_F), because the heat is being taken at a higher altitude where the Reynolds number (R_e) is lower and (C_F) is proportionately increased.

Taking equation (32), we see that

$$Q \sim \int_{\bar{v}_2}^{\bar{v}_1} \frac{\bar{v}^3}{Z^{\frac{1}{2}} \cos^2 \theta} \, d\bar{v}.$$

If $\cos\theta \simeq 1$ and taking arbitrarily the upper limit $\bar{v}_1 = 0.99$, it is possible to calculate the values of this integral for various lift/drag ratios. On the basis of equation (33), Z is taken as being equal to

$$\frac{1 - \bar{v}^2}{\bar{v}\sqrt{\beta r}\,\frac{L}{D}} .$$

A table of some values thus calculated follows:

L/D	$\int_{\bar{v}_2}^{\bar{v}_1} \frac{\bar{v}^3}{Z^{\frac{1}{2}}}\, d\bar{v}$
-1.0	0.75
-0.5	0.93
-0.25	1.09
-0.1	1.23
0	1.36
0.1	1.54
0.25	1.90
0.5	2.53
1.0	3.54

The foregoing discussion presented a practical theory of reentry thermodynamics and a few examples of its application. The number of possible applications is very large (e.g., where $\cos\theta \neq 0$ for glide reentry, $\frac{d\theta}{dt} \neq 0$ for a ballistic vehicle, etc.). Some of these specialized cases have been solved, while others require extremely complex analysis and are best handled empirically or approximated by appropriate simplifying assumptions. Some interesting discussions of specialized problems and their solutions may be found in references 21, 24, 26, 28, 40, 45, 54, 58, 81, 96, 109, 114, 125, 141, 142, 200, 205, 207, 221 and 231.

4. DECELERATION

The second most serious problem facing a reentry vehicle is that of deceleration. As the vehicle strikes the atmosphere in its trajectory toward the surface of the earth or other planet, it is possible that very strong forces may be developed owing to aerodynamic drag. Unless controlled, the drag could be considerably greater than the opposing force caused by the earth's gravitational field, and this could cause an appreciable negative acceleration. The purpose of this section is to discuss the various methods of reentry, their effect on deceleration and methods of predicting the deceleration at any point in the trajectory of reentering vehicles. Again, as in the case of aerodynamic heating (section 3), the following mathematics is largely based on the equations of motion presented in section 2.4.1.

The basic equation for deceleration with respect to a vehicle entering the atmosphere directly from a parabolic orbit can be obtained from the general equation of motion (section 2.4.1):

$$\frac{dv}{dt} = g \sin\theta - \frac{\rho v^2}{2m}(C_D A). \tag{39}$$

By making certain assumptions, that--

(a) $\frac{d\theta}{dt} = 0$

(b) C_D is constant,

(c) the gravitational force is small compared to drag and

(d) there is no lifting force (i.e., ballistic design),

equation (39) reduces to

$$\frac{dv}{dt} = -\frac{C_D A \rho v^2}{2m}. \tag{40}$$

In section 2.3 we saw that $\frac{\rho}{\rho_{SL}} = e^{-\gamma\beta}$ or that $\rho = \rho_{SL}\, e^{-\gamma\beta}$.

Then if $\sigma = \frac{\rho}{\rho_{SL}}$ we have for the reentering vehicle

$$\sigma = \frac{\rho}{\rho_{SL}} = e^{-\gamma\beta}. \tag{41}$$

The instantaneous condition for the reentering vehicle can be represented as follows: $$y = y_1 - v t \sin\theta \tag{42}$$

where t is a very short time period (or Δt) and y_1 is the initial altitude when t = 0. Therefore, for the instantaneous condition, σ is seen to be a function of time, or

$$\sigma = e^{-\beta(y_1 - v t \sin\theta)} = e^{-\beta y_1} e^{\beta v t \sin\theta} \tag{43}$$

Differentiating with respect to t, we have

$$\frac{d\sigma}{dt} = \beta v \sin\theta\, e^{-\beta y_1} e^{\beta v t \sin\theta} \tag{44}$$

on the basis that v is constant during the short time interval. Since $e^{-\beta y_1} e^{\beta v t \sin\theta} = \sigma$ from equation (43) we have

$$\frac{d\sigma}{dt} = \beta v \sigma \sin\theta. \tag{45}$$

Eliminating dt between equations (40) and (45),

$$\frac{dv}{d\sigma} = -\frac{C_D A \rho v^2}{2m\beta v \sigma \sin\theta} \tag{46}$$

From equation (41), $\rho = \sigma \rho_{SL}$, and (46) reduces to

$$\frac{dv}{d\sigma} = -\frac{C_D A \sigma \rho_{SL} v}{2m\beta\sigma\sin\theta} = -\frac{C_D A \rho_{SL} v}{2m\beta\sin\theta} \tag{47}$$

or

$$\frac{dv}{v} = -\frac{C_D A \rho_{SL}}{2m\beta\sin\theta}\, d\sigma. \tag{48}$$

Integrating between the appropriate limits

$$\int_{v_{ESC}}^{v} \frac{dv}{v} = \int_{0}^{\sigma} -\frac{C_D A \rho_{SL}}{2m\beta\sin\theta}\, d\sigma \quad \text{and}$$

$$\log \frac{v}{v_{ESC}} = -\frac{C_D A \rho_{SL} \sigma}{2m\beta\sin\theta}$$

or

$$\frac{v}{v_{ESC}} = e^{-\frac{C_D A \sigma \rho_{SL}}{2m\beta\sin\theta}}. \tag{49}$$

Then the deceleration

$$\frac{dv}{dt} = -\beta v_{ESC}^2 \sin\theta \left(\frac{C_D A \rho_{SL} \sigma}{2m\beta\sin\theta}\right) e^{-\frac{C_D A \rho_{SL} \sigma}{m\beta\sin\theta}} \tag{50}$$

and

$$\frac{dv}{dt} = -\beta v_{ESC}^2 \sin\theta \left(\frac{v}{v_{ESC}}\right)^2 \ln \frac{v}{v_{ESC}} \tag{51}$$

Taking the escape velocity ($\sqrt{2gR}$) and differentiating the right side of equation (51) with respect to v and equating to zero, it is possible to find the point of maximum deceleration, or $\left(\frac{dv}{dt}\right)_{MAX}$.

This calculation yields the result $\left(\frac{dv}{dt}\right)_{MAX} = -\frac{\beta R g \sin\theta}{e}$ (52)

or $v_{MAX} = 0.607 v_{ESC}$ by taking $\sin\theta = 1$.

Equation (52) indicates that maximum deceleration could occur when the velocity of vehicle reentering on a parabolic trajectory reaches a velocity of 0.607 v_{ESC}, or approximately 22,500 fps. On the other hand, from equation (49) we see that the velocity at any given altitude where σ assumes a definite value, say σ_K, is

$$v = \frac{v_{ESC}}{e^{\frac{C_D A \rho_{SL} \sigma_K}{2m\beta\sin\theta}}} . \qquad (53)$$

It is obvious from equation (53) that the actual velocity at that fixed altitude will depend on the value of the factor $\left(\frac{C_D A}{m \sin\theta}\right)$. We can then conclude that, for large values of C_D and small values of m and $\sin\theta$, peak deceleration will occur at higher altitudes. Since it is intuitively clear that high rates of heating occur when high velocities persist to relatively low altitudes where the atmosphere is dense, this result is in agreement with the conclusions formed from equation (36), in which we saw that

$$\dot{q}_{MAX} \sim \sqrt{\frac{m}{C_D A R}} .$$

It is also obvious from equation (53) that a shallow path (small angle of entry) results in peak deceleration at higher altitudes. At the same time it should be noted from equation (52) that the maximum deceleration rate is independent of vehicle characteristics (C_D and m) but is influenced only by the angle of entry.

Next, it is desirable to consider the fundamentals of deceleration that occurs when a vehicle enters the atmosphere from a decaying circular orbit. It has been established that the circular velocity

$$v_c^2 = Rg \qquad (54)$$

and

$$v_c^2 = \frac{1}{2} v_{ESC}^2 . \qquad (55)$$

Also, we know from section 2.4.1 that

$$-\frac{dv}{dt} = -g\sin\theta + \frac{\rho v^2}{2m}(C_D A). \tag{56}$$

Differentiating equation (54) with respect to time and inserting the result in (56), we have

$$\frac{C_D A \rho}{2m} = \frac{\sin\theta}{2r}$$

or

$$\sin\theta = \frac{C_D A \rho r}{m}. \tag{57}$$

Replacing for $\sin\theta$ in equation (56)

$$-\frac{dv}{dt} = -g\frac{C_D A \rho r}{m} + \frac{\rho v^2 C_D A}{2m}$$

since from (54) $v^2 = rg$ and

$$-\frac{dv}{dt} = -g\frac{C_D A \rho r}{m} + \frac{\rho r g C_D A}{2m}$$

or

$$\frac{dv}{dt} = \frac{\rho r g C_D A}{2m}. \tag{58}$$

Equation (58) indicates that in this regime the vehicle is accelerating as potential energy is being converted into kinetic energy, while the drag is insufficient to convert any significant amount of this transfer energy into thermal energy. As the altitude decreases and density of the atmosphere increases, however, a point will be reached at which the acceleration is reduced to a zero value; after that, it becomes negative. When the drag becomes appreciable, it is necessary to make certain simplifying assumptions in order to obtain an equation for deceleration. According to reference 215, these can be summarized as follows:

(1) $g\sin\theta \ll \frac{dv}{dt}$

(2) $v\sin\theta \simeq$ constant

(3) $\sin\theta \simeq 0$

(4) $\cos\theta \simeq 1$

From the third assumption we have that equation (56) can be reduced to

$$-\frac{dv}{dt} = \frac{\rho v^2}{2m}\left(C_D A\right).$$

Also, the second equation of motion in section 2.4.1,

$$\frac{v}{\cos\theta}\frac{d\theta}{dt} = g - \frac{v^2}{r} - \frac{\rho v^2}{2m\cos\theta}\left(C_L A\right) \tag{59}$$

becomes

$$v\frac{d\theta}{dt} = g - \frac{v^2}{r} \tag{60}$$

since it is assumed that $C_L = 0$.

If $\sigma = \frac{\rho}{\rho_{SL}}$ these equations can be combined to yield

$$-\left(g - \frac{v^2}{r}\right)\frac{dv}{d\sigma} = \left(\frac{C_D A \rho_{SL}}{2m}\right)^2 \frac{\sigma v^3}{\beta} \tag{61}$$

and integrating between limits $(0,\ v_c)$ and (σ, v)

$$\ln\left(\frac{v}{v_c}\right)^2 + \left(\frac{v_c}{v}\right)^2 - 1 = \left(\frac{C_D A \rho_{SL}\sigma}{2m\beta}\right)^2 \beta r. \tag{62}$$

From equation (62) we have the deceleration of

$$-\frac{dv}{dt} = g\sqrt{\beta r}\left(\frac{v}{v_c}\right)^2 \sqrt{\ln\left(\frac{v}{v_c}\right)^2 + \left(\frac{v_c}{v}\right)^2 - 1} \tag{63}$$

Differentiating with respect to v and setting the result equal to zero, we obtain the maximum value of $\left|-\frac{dv}{dt}\right|$ which is computed as

$$\left(-\frac{dv}{dt}\right)_{MAX} = 0.32\, g\sqrt{\beta r}.$$

This value is reached when

$$\frac{v}{v_c} = 0.534.$$

It is interesting to note that, in the case of a circular-orbit decay, the maximum deceleration is independent of vehicle characteristics; this value is governed exclusively by the atmosphere and gravitational field.

The next fundamental situation to be considered is a reentry vehicle have some lifting capacity. It is reasonable to make the following assumptions in this case:

(1) $\sin\theta \ll 1$

(2) $\cos\vartheta \simeq 1$

(3) $\frac{d\theta}{dt} \simeq 0$

(4) $g\sin\theta \ll \frac{dv}{dt}$.

Using these assumptions, equations (56) and (59) can be reduced to

$$-\frac{dv}{dt} = \frac{C_D A \rho_{SL} \sigma v^2}{2m} \tag{64}$$

and

$$\frac{C_L A \rho_{SL} \sigma v^2}{2m} = g - \frac{v^2}{r} \tag{65}$$

where $\sigma = \frac{\rho}{\rho_{SL}}$.

Equation (65) can be solved for v so that

$$v = \left[\frac{g}{\frac{1}{r} + \frac{C_L A \rho_{SL} \sigma}{2m}}\right]^{\frac{1}{2}} \tag{66}$$

Comparing this with v_c previously obtained and replacing in (65), we have

$$-\frac{dv}{dt} = \frac{g\left[1 - \left(\frac{v}{v_c}\right)^2\right]}{\frac{L}{D}}$$

or

$$-\frac{dv}{dt} = \frac{gD\pi C_D A \rho_{SL} \sigma}{L\pi C_D A \rho_{SL} \sigma + 2mD}. \tag{67}$$

From equation (67) we see that $\frac{dv}{dt}$ does not reach a maximum value but increases, continuously approaching the asymptotic value of

$$\left(-\frac{dv}{dt}\right)_{MAX} = \frac{gD}{L} \tag{68}$$

As may have been expected, the characteristics of the vehicle exert a strong influence over the maximum deceleration value during descent. In fact, this value is inversely proportional to the lift/drag ratio. As noted from equation (68) this value is reduced to a single g as the lift/drag ratio approaches unity. Naturally in the selection of designs for a reentry vehicle, deceleration is only one of the factors to be considered. Although from this standpoint increasing the lift/drag ratio may be desirable, it could adversely affect other aspects of reentry. In particular, increasing the lift/drag ratio results in a longer time of descent, with a corresponding increase in total heat transferred to the vehicle and loss of landing-point accuracy. On the positive side, an increase in the lift/drag ratio could improve control during descent and perhaps make it more comfortable for human passengers. While balancing the critical reentry factors in an effort to obtain an optimum design, therefore, the vehicle's special purpose must be considered.

In addition to the foregoing fundamental equations, containing deceleration as the dependent variable, which were developed on the basis of Newtonian physics, it is desirable to relate deceleration to the Z function discussed in section 2. This approach is useful in that it eases the determination of deceleration for specific cases, since the Z function has already been computed for a wide range of shallow reentries of lifting and nonlifting vehicles of arbitrary mass and size having constant aerodynamic coefficients (ref. 48).

It was seen in section 2.4.1 that

$$\vec{a} = \left(\frac{dv_2}{dt} - \frac{v_1^2}{r}\right) i_r + \left(\frac{dv_1}{dt} + \frac{v_1 v_2}{r}\right) i_\theta . \qquad (69)$$

Consequently the magnitude of the acceleration vector can be represented as

$$a \equiv \frac{dv}{dt} = \sqrt{\left(\frac{dv_2}{dt} - \frac{v_1^2}{r}\right)^2 + \left(\frac{dv_1}{dt} + \frac{v_1 v_2}{r}\right)^2} . \qquad (70)$$

In order to solve equation (70), therefore, it is necessary to obtain suitable relationships for the horizontal $\left(\frac{dv_1}{dt}\right)$ and vertical $\left(\frac{dv_2}{dt}\right)$ components of acceleration. From equation (6) (section 2.4.2), we know that, by making certain simplifying approximations,

$$\frac{dv_1}{dt} = \sqrt{gr}\,\frac{d\bar{v}}{dt} \qquad (71)$$

and again from equation (11)

$$\frac{d\bar{v}}{dt} = -\sqrt{g\beta}\,\frac{\bar{v}Z}{\cos\theta}\,. \tag{72}$$

Substituting this value in (71), we have

$$\frac{dv_1}{dt} = -\sqrt{gr}\left(\sqrt{g\beta}\,\frac{\bar{v}Z}{\cos\theta}\right) = -g\sqrt{\beta r}\,\frac{\bar{v}Z}{\cos\theta}\,. \tag{73}$$

Next it is desired to find a value for the vertical component of acceleration. It was seen in equation (18) that

$$-\frac{1}{g}\frac{dv_2}{dt} = 1-\bar{v}^2 + \frac{\bar{v}Z}{\cos^2\theta}\left(Z' - \frac{Z}{\bar{v}} - \sqrt{\beta r}\,\frac{L}{D}\cos\theta\right)$$

or that

$$\frac{dv_2}{dt} = \frac{\bar{v}^2}{g} - \frac{1}{g} - \frac{\bar{v}Z}{g\cos^2\theta}\left(Z' - \frac{Z}{\bar{v}} - \sqrt{\beta r}\,\frac{L}{D}\cos\theta\right). \tag{74}$$

Now relating equations (73) and (74) with equation (70), we have

$$\frac{dv}{dt} = \left\{\left[\frac{\bar{v}^2}{g} - \frac{1}{g} - \frac{\bar{v}Z}{g\cos^2\theta}\left(Z' - \frac{Z}{\bar{v}} - \sqrt{\beta r}\,\frac{L}{D}\cos\theta\right) - \frac{v_1^2}{r}\right]^2 + \left[\frac{v_1 v_2}{r} - g\sqrt{\beta r}\,\frac{\bar{v}Z}{\cos\theta}\right]^2\right\}^{\frac{1}{2}}. \tag{75}$$

A number of important practical results are indicated in the preceding analysis. Equation (75), of course, furnishes the absolute value of the deceleration for a reentering vehicle, but equation (73) is also very significant for shallow reentry, especially in the case of vehicles with an appreciable lift/drag. The reason is that much of the deceleration occurs at high altitudes where the angle θ is small. Consequently, equation (73) can be simplified to

$$\frac{dv_1}{dt} \simeq \frac{30}{g}\,\bar{v}Z \tag{76}$$

since $\cos\theta \simeq 1$.

Also, it is possible to simplify equation (75) by making use of inequality (3) and the six assumptions in section 2.4.2. The result is that

$$\frac{d\upsilon}{dt} = \frac{\sqrt{\beta\pi}\,\bar{\upsilon}Z}{\cos\theta}\sqrt{1+\left(\tan\theta - \frac{L}{D}\right)^2} \quad . \tag{77}$$

From this it is clear that the maximum deceleration value occurs when $\theta \simeq 0$, and then we have

$$\left(\frac{d\upsilon}{dt}\right)_{MAX} \simeq g\sqrt{\beta\pi}\,\bar{\upsilon}Z_{MAX}\sqrt{1+\left(\frac{L}{D}\right)^2} \quad . \tag{78}$$

Thus we see that both L/D and $\bar{\upsilon}$ are strong influences over the maximum deceleration during reentry. Plotting $\left(\frac{d\upsilon}{dt}\right)$ vs. $\bar{\upsilon}$ for various fixed values of L/D, it has been determined that maximum deceleration occurs when $\bar{\upsilon} \simeq 0.5$ and that it tends to increase with decreasing values of L/D. Some peak deceleration values are given in the following table.

$\left(\frac{d\upsilon}{dt}\right)_{MAX}$ (g)	L/D
0.9	1.0
1.6	0.5
2.7	0.25
4.9	0.1
8.4	0
12.7	-0.1

5. COOLING TECHNIQUES

5.1 Introduction.

As stated in section 3, the total amount of heat transferred to a reentering body as it passes through the atmosphere is so large and the heat-transfer rate is so high that this problem demands special attention. This consists of designing the vehicle so that reentry causes neither unacceptable structural damage nor temperatures in any part of the vehicle that exceed established limits.

Several ways of dissipating absorbed heat during reentry have been considered, including (1) reflectance, that is, electromagnetic radiation away from the vehicle; (2) transpiration (or chemical) cooling by the use of various materials, usually fluids carried inside the vehicle, that are spread over the surface to form a heat-absorbing boundary layer; (3) ablation, that is, a coating on the reentry vehicle's surface consisting of materials (such as ceramics) that remove heat by vaporizing under intense heat and pressure; and (4) the heat sink, a mass carried within the vehicle whose temperature rises as it absorbs heat. These and other possible, but unproved methods are discussed in this section. The information presented here is based on references 2 through 19 and 29, 31, 43, 79, 88, 94, 124, 138, 139, 140, 143, 144, 145, 150, 164, 190, 191, 192, 201, 206, 232, 235, 236, 238, 243, 244, 246, 247, 253, 254, 256, 257, 259, 260 and 262.

5.2 Reflectance.

The term "reflectance," as used for reentry cooling, may not be entirely descriptive of the function. Essentially the process of reflectance is the dissipation of energy by electromagnetic radiation away from the vehicle. Furthermore, most of the heat taken in by the vehicle is generated by a thermal convective process; relatively little heat is absorbed by radiation. Consequently "reflectance," implying a ratio of the reflected radiant flux to the incident radiant flux, does not apply to reentry cooling. Probably the term has been used because it is very descriptive of other phases of motion in outer space, where the primary source of incident energy is solar radiation and a reflectance cooling process is therefore essential over long periods of time. In any event, "reflectance," as used here, applies to all forms of cooling by radiation.

At first glance it is obvious that reflectance is the most desirable method of reentry cooling, primarily because this process imposes no

weight penalty on the reentering vehicle. The several layers of radiative surface would probably comprise the required outer shell for the vehicle. Since reflectance involves no loss of material, it would be possible to combine the cooling system with the vehicle's normal structural requirements. All other methods of cooling require the addition of relatively heavy components to the reentry-vehicle design--ablation shields, heat-sink masses, etc.

A practical investigation of the reflectance process indicated that molybdenum and tungsten are probably the most suitable materials for this use. Thin sheets of such materials, backed by highly polished layers of other metals such as aluminum, could dissipate heat by radiation at a relatively high rate.

Despite all the attractions of reflectance cooling, there appear to be a number of weaknesses in this method that have not yet been overcome. Experiments have indicated that cooling by reflectance is too slow in relation to the high rate of heating developed in a large-angle-of-entry ballistic trajectory. Also, at this time, the bonding (usually rubber) between layers cannot withstand temperatures much above 1800°C, while reflectance cooling does not attain maximum efficiency until somewhat higher temperatures are reached; during ballistic reentry, temperatures of 2500°C are not uncommon. Nevertheless, for reentry vehicles with $C_L > 0$ and for certain low-angle-of-inclination satellite reentries, it is probable that reflectance will prove to be the most satisfactory cooling method, especially after more research is done in this area and some of the engineering difficulties are overcome.

5.3 Transpiration Cooling.

It is possible to cool a heated surface by forcing a fluid through one or more openings in it. For bodies in relative motion with respect to the surrounding air, the injection of the cooling fluid should be in the forward region of reentry. There will be a cooling effect, first, as the fluid absorbs heat on reaching the surface and, then, as a protective boundary layer is formed downstream from the injection point. This technique, known as transpiration cooling, has been studied recently by several investigators (ref. 30, 194, 196). Some of the work has been done in connection with projects to develop cooling methods for interior surfaces such as the jet engine, rocket-nozzle throat, etc., which are subject to supersonic air flow. Many of the results are also applicable to the cooling of reentry-vehicle surfaces.

In the best understood process of transpiration cooling, small quantities of relatively cold gas are injected through a porous surface in the forward section of the reentry vehicle. The injection, of course,

should be applied in the region of the most severe heating, such as the nose of an axisymmetric body. It is also very important to know the anticipated maximum reentry velocity for any given design because of the effect of shock waves on the downstream boundary-layer cooling. The wave angle and the regions where the shock waves are formed (such as points of discontinuity on the surface) are likely to influence the effectiveness of transpiration cooling for any particular design. Thus it may be desirable to inject only small quantities of gas in the stagnation section, while extending the porous surface beyond the limit of the shock-wave burble, in this way ensuring some boundary-layer effect toward the rear of the vehicle.

Up to now, some of these problems have been disregarded in most research and experimentation, and attention has been concentrated on the decay of the cooling effect with increasing distance downstream from the injection region. This was based on the zero-pressure-gradient assumption; the gases used were air and helium. The results of this work are shown in Figures 8 and 9.

Theoretical work on transpiration cooling has shown (ref. 30) that the wall-cooling parameter

$$\left(\frac{T_w - T_c}{T_{aw} - T_c} \right)$$

is a function of the downstream distance, injection rate and Prandtl number. An exact mathematical relationship between these variables could then be established, but it would only be applicable to a flat plate and would be based on the assumption that no shock waves were formed to disturb the boundary layer. Each practical design would have to be tested to establish this relationship for that particular case. Furthermore, since shock wave forms will vary as the velocity changes, the results would only hold for specific velocity regions.

In analyzing results obtained experimentally (ref. 196) by measurements taken to correspond to four distance parameters where

$$\overline{X} = \frac{X - X_i}{X_o - X_i}$$

it was found that, when plotting the wall-cooling parameter to distance-parameter ratio vs. wall-injection parameter ratio vs. wall-injection parameter on a log-log plot, the curves were, in fact, straight lines. Here the wall-injection parameter

$$P = \frac{(\rho v)_w}{(\rho u)_o} \sqrt{Re_o} .$$

FIGURE 8

THE EFFECT OF INJECTION RATE ON DOWNSTREAM SURFACE TEMPERATURE

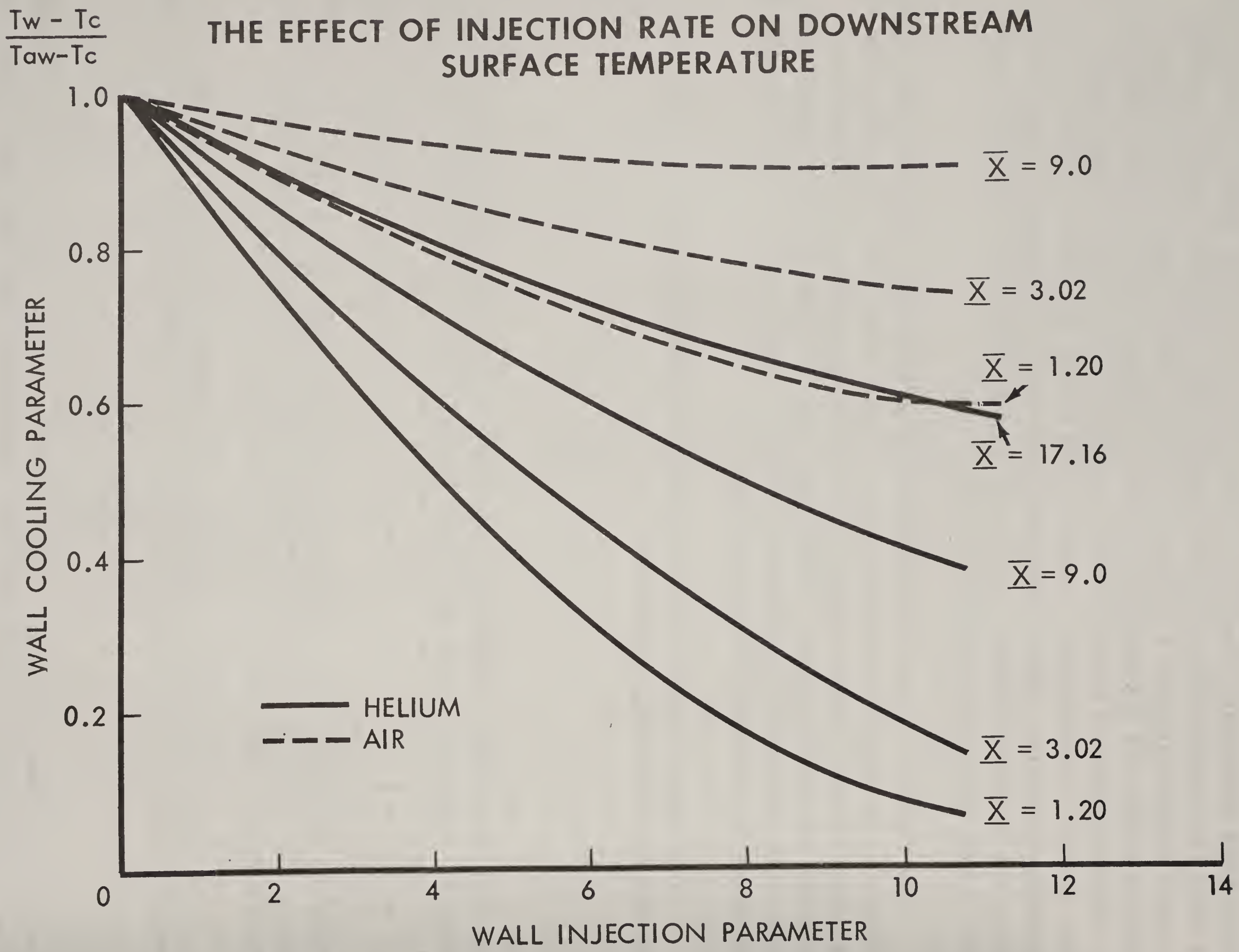

FIGURE 9

SURFACE-TEMPERATURE DISTRIBUTIONS FOR SEVERAL INJECTION RATES

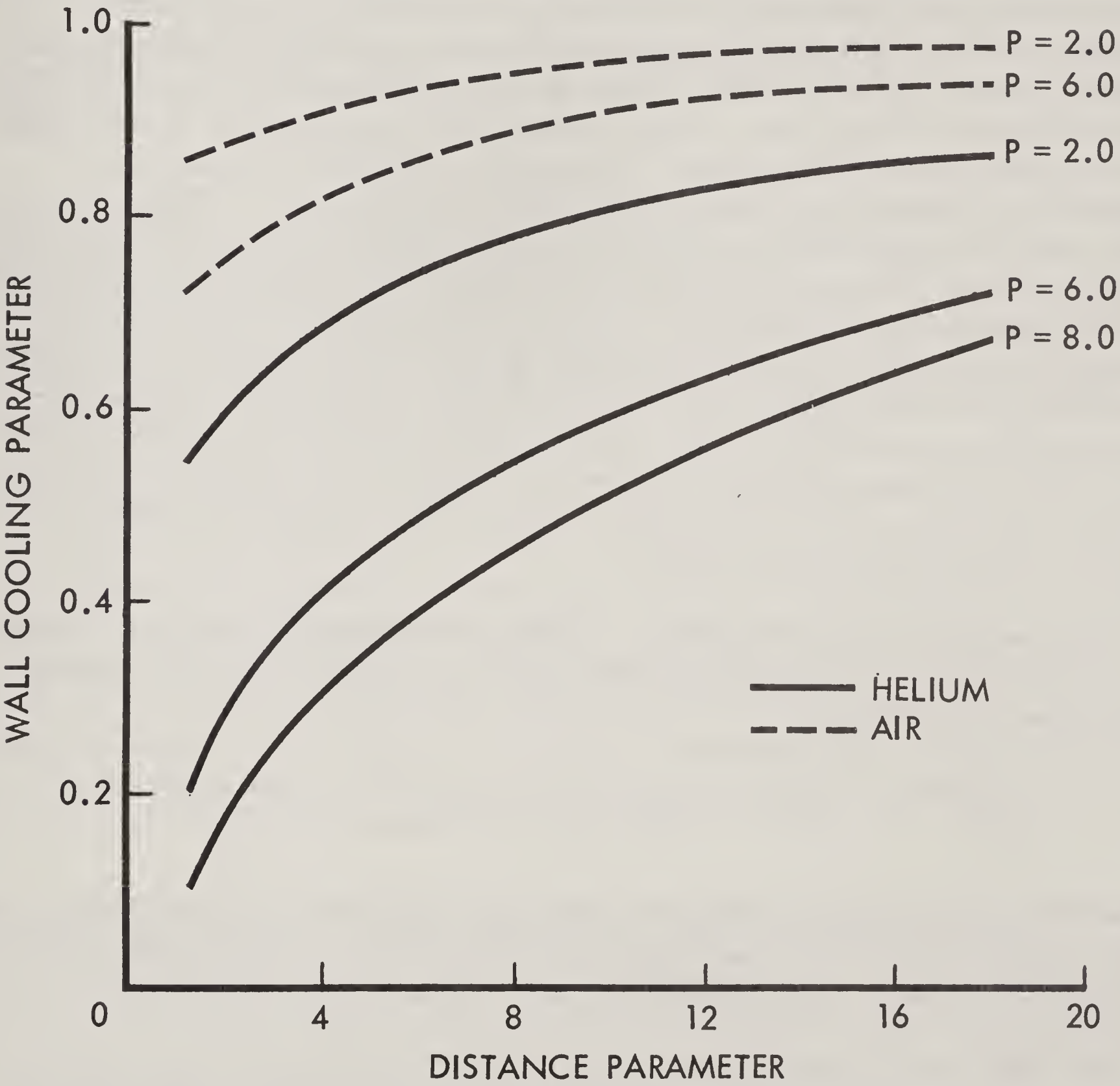

This indicates that the wall-cooling parameter is proportional to a power of the distance parameters, the exponent being separable into a product of the wall-injection parameter and a constant that depends on the particular gas used for cooling. This conclusion can then be summarized mathematically as follows:

$$\frac{\overline{T_w} - \overline{T_c}}{\overline{T_{aw}} - \overline{T_c}} \sim \overline{\overline{X}}\, K_c P^{\frac{3}{4}}$$

5.4 Ablation.

One of the most widely used methods for protecting the ballistic reentry nose cone from heat is ablation, a process in which the absorbed heat is dissipated as the mass of the specially constructed protective outer cover is lost. Heat is first absorbed by the protective cover acting as a heat sink. Then, when the temperature in the outer layer reaches the melting point, substantial amounts of heat are absorbed in changing the state of the ablation material. Thus, heat of fusion, heat of sublimation and heat of vaporization serve as important cooling factors. The air stream then carries the molten and vaporized material away from the vehicle. Much of this material then forms a boundary layer along the rear sections of the vehicle and so provides some heat protection against the free-stream conditions. Moreover, as most ablation materials have relatively low thermal-conductivity rates, the remaining ablation layers, by implication, also serve as a protective barrier to heat moving by conduction toward the critical sections of the reentering vehicle.

The mathematics of ablation cooling is extremely simple. The rate of heat absorbed and remaining with the ablation surface can be represented as follows:

$$\frac{dQ_1}{dt} = \frac{dQ_2}{dt} - m C_1 - m C_2 - \frac{m Q_2}{M}$$

where Q_1 is the amount of heat remaining, Q_2 is the total heat absorbed by the vehicle, M is the total mass of the vehicle, m represents the rate of loss of mass through melting and vaporization, that is, $m = \frac{dM}{dt}$, C_1 the heat of fusion and C_2 the heat of vaporization.

Although an analytical approach to ablation is possible--and usually profitable--before initiating a design, there are a number of

practical engineering problems that must be carefully considered, and then models or prototype vehicles must be extensively tested.

Problems that should be considered include possibilities that protective layers might be delaminated prematurely, thermal stresses in the ablation material may be excessive, and protective material in the envelope may be distributed unsatisfactorily. For example, it was found that the orientation of the glass fiber with respect to the exposed surface significantly influenced the occurrence of delamination. When the fiber was normal to the direction of heat flow, the laminating resin frequently decomposed before the glass melted. On the other hand, when the fiber was parallel to the heat flow, this did not happen. Delamination of this type can be critical for a reentering vehicle because large chunks of ablation material will be lost before it can perform its mission and also because the consequently uneven outer surface results in turbulence, shock waves and further loss of heat-absorption potential.

Among the materials used for ablation are plastics, fiber glass and ceramics. Most of the research on materials was done in connection with reentering ballistic-missile nose cones and the resulting information is classified; furthermore, it would not add significantly to a theoretical understanding of reentry physics. Detailed information on ablation materials may be found in some of the references listed in the bibliography to this report.

5.5 The Heat Sink.

One of the methods of cooling a reentry vehicle that was first studied was the so-called heat sink. In this method a large volume of material is required to absorb the heat generated by reentry. The heat-sink material is best distributed around the nose cone where it absorbs heat in the region of maximum transfer rate and so prevents excessive heat from reaching critical points such as instrumentation, electric circuits and mechanical systems.

A material used as a heat sink must satisfy certain requirements, of which the most important are the possession of high thermal conductivity, high specific heat and a high melting point. Of several materials used in heat-sink experiments, the most effective thus far is copper. Graphite was also considered because of its high melting point and other heat-absorptive qualities, but it is very hard to use owing to the presence of voids and other structural defects. The method considered for using graphite as a heat sink was to cast the material in large blocks and then machine the protective coat to shape. Because of the structural defects, however, this process has not worked well.

The dissipative capacity of a heat sink can be represented mathematically as follows:

$$Q_2 = c\left(T_1 - T_2\right)W$$

5.6 Possible New Methods of Cooling.

In addition to those discussed before, there are several possible methods of cooling the surface of reentering vehicles. Some have been partially investigated, while others are still in the stage of speculation. Four of these methods are briefly described in the following subsections.

5.6.1 Thermal Insulation: The objective here is to develop materials that, when used in coating critical areas of the vehicle's surface, will significantly retard the transfer of heat beyond the outermost layer. The two most important qualities these materials must possess are very low thermal conductivity and the ability to withstand extremely high temperatures without melting or fracturing.

Thermal insulation for the protection of reentry vehicles has been investigated to a considerable extent. Of several materials tested for this purpose, the most suitable have consisted of various ceramics, but they did not satisfy the minimum standards set by the Federal Government's program of reentry research. The search for more acceptable materials is still proceeding, and a technical breakthrough in this area is quite possible.

If the right material can be found, the use of thermal insulation appears to have a number of advantages. In particular, it would permit the construction of relatively thin protective coatings for reentry vehicles, almost certainly a significant advantage in weight over any other cooling technique--possibly even reflectance. At present the search centers around carbide, boride, nitride and silicide cermets, all of which are strong and have high melting points and chemical stability.

The materials tested so far have failed principally because of thermal shock. These ceramics have very good compression strength but are usually weak with respect to tension. The thermal shock causes unequal expansion; this results in considerable shear and tension stresses, which frequently cause separation and fracturing.

5.6.2 Internal Cooling: Theoretically it would be possible to cool the surface of a reentering vehicle by circulating a coolant through a dense network of tubes immediately below the vehicle's surface. It might also be possible to keep the coolant in motion between two layers

in the outer surface. The internal cooling method would then be comparable to systems used in the rocket nozzles of liquid-fueled engines.

A number of technical difficulties are associated with the internal cooling system. The coolant would have to be circulated very rapidly during peak heating periods. It would be necessary to dissipate the absorbed heat (1) by transferring it from the fluid at some point in the cycle or (2) disposing of the fluid, either permanently, by dumping, or by temporarily removing it from the system until it cools. Either alternative presents certain problems. It would be difficult to accomplish the first, while the second would greatly add to the cooling system's weight.

In any case, with internal cooling, the reentry vehicle would be loaded with the coolant, a pump or pressure mechanism to circulate it and the necessary heat-transfer equipment. Moreover, the internal-cooling method is limited by the low boiling temperature of liquids as compared to that of solids used for reentry cooling, e.g., ablation.

Although internal cooling appears to have a number of weaknesses, it is still a potentially useful method and its investigation should continue. In view of the similarity of this method and the heat sink, the two approaches might be combined for purposes of research and testing.

5.6.3 Chemical Surface Reaction: In one test of this technique, a wood shield was used. The wood had been soaked in water and secured to the vehicle so that its grain pointed away from the envelope, causing the air flow over the cone to be orthogonal to the grain. When the temperature at the surface rose high enough, the water in the wood was forced toward the surface where it evaporated. After about 20 seconds of very high temperature, all the water was drained out and the wood started to burn.

It is clear that this use of wood for cooling is not satisfactory, since the chemical reaction during the burning process would tend to increase the total heat generated. The use of some similar material, however, which would not burn but perhaps would ablate when all the fluid had separated as the result of chemical reaction, might be acceptable. Materials soaked in aqueous salt solutions were also investigated on the assumption that heat would be absorbed during the decomposition of sodium chloride and the evaporation of the water of crystalization. As the results have not been very conclusive, additional research, including the use of other materials, is probably justifiable.

5.6.4 Point Mass Addition: In this method, a fluid is introduced at or near the stagnation point of the reentering vehicle. As the fluid

vaporizes, it absorbs heat, which is then carried away by the air stream. In principle, the method is similar to transpiration cooling, although larger amounts of fluid are ejected through a smaller area of the vehicle's surface.

5.7 Testing and Simulation.

As indicated in section 3, it is possible to predict with reasonable accuracy both heating rates and total heat created by a space vehicle during reentry. Further, a number of techniques for dissipating this heat (sections 5.1 through 5.6) are available. Although a theoretical approach to the cooling problem, which is always desirable, may produce a fundamental breakthrough in this difficult engineering problem, it should be recognized that the effectiveness of any given technique cannot be predicted with any degree of certainty. The reason for this is that various materials, when exposed to combinations of thermal shock, nonuniform expansion, strong aerodynamic forces, turbulence, etc., may have unexpected reactions. Only by realistic testing can a reasonable assurance be obtained that a particular cooling system is, in fact, effective. The test objective can be attained, using full-scale vehicles or models, by actually propelling the vehicle beyond the earth's atmosphere and observing reactions on reentry or by simulating reentry with appropriate equipment on the ground.

There are disadvantages in both methods. Experiments involving actual reentries pose the problem of recovering the vehicle. In addition, any failure of the cooling system could easily cause extensive damage to the vehicle, making it impossible to establish the cause of failure. This, then, would prevent necessary corrective action--which actually might only be minor design changes in the cooling system. It is relatively difficult to control the actual reentry of a space vehicle, for the trajectory may not turn out as predicted; also the experiment cannot be stopped at any time for the purpose of acquiring a better understanding of the process.

The main disadvantage of the simulation technique is that conditions are never exactly comparable to those of an actual reentry. There are likely to be variations not only in the heating rate but in the density of the surrounding gas, the reentry velocity and the free stream's chemical composition. All these factors significantly affect the performance of the cooling system. Nevertheless, some simulation tests are necessary to provide data that can serve as a basis for deciding whether to embark on full-scale reentry experiments.

The Federal Government has developed a number of facilities for experimenting with reentry conditions. Since some of the detailed

specifications may still be classified for security purposes, this paper only discusses in general terms the principles governing the facilities' construction.

In the most useful simulation testing method, rocket motors are used. Through proper control of the rockets, it is possible to carefully control a number of parameters, including pressure, exhaust-gas composition, velocity and--most important--temperature and heating flux. Temperatures well over 6000°K and heating rates of over 2000 Btu per square foot have been reached. Velocities have varied in the test chambers, but they were usually below Mach 4.

The high-intensity electric arc has been studied as a possible method of simulating reentry conditions, but it did not prove to be particularly useful.

The reentry environment can also be simulated in the laboratory by using a straight shock tube in which a removable diaphragm separates a gas at high pressure from the air surrounding the test model. When the diaphragm is very quickly removed, a shock wave is produced which compresses the air, heats it and sets it in motion at a velocity comparable to that of a reentry shock wave. Even higher pressures can be produced by combustion methods. The heat transfer and pressure can be measured with appropriate sensory equipment. This type of test has a limited value because of the shock wave's very short duration.

Supersonic air jets have also been used in testing reentry models. The main advantage of using this equipment is in comparing the results with those obtained from rocket motors, in which the stream composition is different from that normally encountered in air.

6. SPACE-VEHICLE CONFIGURATIONS

All reentry space vehicles can be classified in two broad groups --those with no lift and those with $L/D > 0$. Each category includes many types and subtypes. This section briefly describes some of these designs and mentions a few of the advantages and disadvantages associated with each.

The nonlifting vehicle could be spherical, a spheriod or what is more commonly called the ballistic shape (the forward or payload section of a rocket or missile). The Mercury space vehicle is a typical ballistic shape. This design has one special advantageous quality--it can have a very high drag coefficient. The ballistic shape also causes an appreciable reduction of convective heating during reentry, which permits a lighter weight cooling system, e.g., ablation material. There are limitations, however, on the permissible drag coefficient for any given vehicle. Increasing the drag coefficient would cause the vehicle to decelerate during certain stages of reentry--and, as indicated previously, deceleration could be a limiting factor on the design because of human passengers or sensitive equipment inside the vehicle.

Construction principles and materials suitable for use in connection with ballistic configurations have been carefully investigated because of their importance to the successful development of missiles. A considerable amount of literature on this subject is available, most of it protected by security classifications because of the military significance of such information. Good summaries of this subject may be found in reference 3.

In two classes of reentry vehicles, $C_L > 0$. The first is a fixed design with a constant C_L for any given angle of attack. The second is a variable-geometry configuration. Several fixed designs have been tested, and a considerable volume of theoretical data is available, some of which has been touched upon in earlier sections of this report.

The variable-geometry concept, although not new, has not been tested to any appreciable extent. A number of variations on this approach have been described in technical papers. One such proposal calls for folded wings on the leeward side of a relatively compact vehicle. After the vehicle has slowed down and reached a low altitude, the wings are unfolded to provide the control and stability needed for a soft landing. Under certain conditions it may be desirable to make

a skip reentry into the earth's atmosphere, which would call for alternately positive and negative lift coefficients until the velocity is lowered by drag forces. This kind of performance is made possible by either inverting the entire vehicle periodically or controlling the angle of attack of the lifting surfaces, producing a variable-geometry configuration. Another advantage of a vehicle that has an appreciable airfoil surface is the possibility that such a surface could be adapted to a radiation (or reflectance) cooling system. Thus, the lifting surface could serve a dual purpose and could even reduce the over-all weight requirements for a special-purpose vehicle.

In the design of a vehicle that is intended to reenter the atmosphere of the earth or another planet, a number of factors must be taken into account. It is important, for example, to know whether the vehicle is to have any form of guidance system. The objective of reentry is assumed to be the arrival of the vehicle at a particular point on the earth's surface or to rendezvous with another vehicle at a relatively low altitude in the atmosphere. If it has no guidance system, the vehicle must depend entirely on the forces that act upon it during the precalculated trajectory. Thus it is perhaps best that the vehicle have no lift since unexpected variations in such parameters as density and wind velocity are likely to affect the trajectory of a lifting vehicle more seriously than they would a ballistic type. On the other hand, a guidance and control system can correct for any unexpected deviation of the vehicle from the prescribed path of descent.

How the vehicle is to be recovered is another important consideration. If it is to be retrieved from a body of water, its specific gravity must be less than 1. A vehicle intended for a soft landing on earth could either use a parachute to reduce its terminal velocity or make some kind of controlled landing, as in conventional aircraft.

Until a vehicle's maximum reentry velocity and trajectory are specified, the exact form of the lifting surface cannot be prescribed. As the speed mounts, it becomes increasingly difficult to provide suitable lift because of the severity of heating conditions. In these circumstances, it is often necessary to compromise control requirements and design a more compact vehicle with a lower lift/drag ratio. Here is an example in which the variable-geometry configuration would be particularly desirable: The vehicle could have a low-lift/drag-ratio shape while traversing regions of severe heating; then later, when its speed is reduced to within safe limits and control is needed for a soft landing, increased lift could be provided.

Special attention must be given to the reliability of control systems and to the heating and stresses that are likely to affect their

performance. If the vehicle is required to maneuver sharply, or if the drag force is suddenly increased a good deal, the situation could become especially critical. Extremely high-temperature gas caps have been known to form around control surfaces. A reasonable margin of safety, therefore, should be built into every control system, particularly in the case of vehicles that are expected to carry humans.

7. CONCLUSIONS

The physics of atmospheric reentry is an essential part of modern space science. Although it would be desirable to perfect the theoretical aspects of this subject, the practical requirements of space travel will be satisfied by approximate results and empirically verified principles. This acceptance of something less than perfection is fortunate, because the field of reentry mechanics and thermodynamics is extremely complex.

Up to now it has been impossible to develop mathematically ideal solutions for variables--such as heating rate and peak deceleration--that could be obtained for any reentry condition merely by inserting appropriate values in a general equation. Instead, it has been necessary either to sacrifice accuracy by using certain simplified general equations or, if greater precision is needed, to develop specialized equations applicable only to a very narrow range of reentry conditions.

As further research is performed, some of these deficiencies will probably be overcome. In fact, one noted scientist stated recently that he is now completing work on "... a second order theory to provide a single analytical approximate solution which can be applied to the entire region of entry." The objective, of course, is to improve on the accuracy of previously developed general solutions. Whether or not this particular effort proves successful, there is little doubt that we can expect major steps forward in understanding reentry mechanics, provided that this effort continues to receive necessary support.

In addition to the general conclusion just briefly stated, it is possible to reach a number of specific conclusions on the basis of the information presented in this paper; they can be summarized as follows:

(1) Vehicles reentering the earth's atmosphere from space are expected to travel at high velocities. The lowest probable reentry velocity would be that of an earth satellite in a decaying orbit, which would be over 25,000 feet per second.

(2) Much of the energy contained in a reentering vehicle by virtue of its altitude and velocity must be converted into heat before it can make a soft landing on the earth's surface.

(3) For purposes of reentry mathematics, it may be assumed that the earth's atmosphere varies exponentially with altitude.

In order to solve numerical problems it may be assumed that a body enters the atmosphere when it drops to an altitude of about 300,000 to 400,000 feet.

(4) The trajectory of a reentry vehicle is a very important factor in controlling such variables as deceleration and heating. Another important factor is the lift/drag ratio. Although increasing this ratio tends to reduce peak deceleration value and peak heating, it has the undesirable effects of increasing total heat and reducing landing accuracy. The trajectory and design of a vehicle can only be selected on the basis of the specific missions for which it is intended. Two important considerations must be kept in mind at all times: (1) The surface temperature has to be kept below a certain maximum value, which will depend on the cooling technique used. (2) The peak deceleration should be limited. If there are humans in the vehicle, the peak deceleration should be held below 10 g; otherwise, the sensitivity of equipment on board determines the maximum permissible deceleration.

(5) Considerable attention must be devoted to the cooling techniques used with various reentry vehicles. Insufficient amounts of cooling material could well cause disaster during reentry, while an excessive amount would reduce the payload capacity for other purposes. Moreover, any improvement in cooling techniques, such as the development of greater efficiency and the reduction of weight, would have obvious advantages.

(6) Every cooling technique should be carefully tested before it is used on a space vehicle. There might be all kinds of unexpected developments, that could cause failure--the bonding material is often unsuitable; thermal shock could have serious consequences. Before a cooling technique is accepted, it would be desirable to conduct both ground tests and tests under actual reentry conditions.

(7) Reflectance holds the greatest promise of efficient cooling, but much more work remains to be done before this technique would be suitable for most reentry-vehicle designs. At present, the outstanding weakness of this method is that reflectance alone cannot dissipate heat fast enough under certain reentry conditions.

(8) In the current state of the art, ablation is the most satisfactory cooling technique for most reentry vehicles. The ablation shield absorbs heat through fusion, sublimation and vaporization. In addition, the residue of the ablation material forms a protective boundary layer along the rear sections of the vehicle.

(9) The use of gas for transpiration cooling is not the most efficient process. One way to improve this method would be to use a liquid in such a way that vaporization occurred in the porous region just below the surface. There would be an additional cooling effect from the fluid's absorption of the heat of vaporization. It is important that only gas reach the surface. Otherwise turbulence would be caused, and that would lessen the cooling effect of gas in the boundary layer downstream from the injection point. The only way to achieve this would be by extremely sensitive injection control, based on surface temperature. Additional research and experimentation in connection with transpiration cooling techniques would probably be very worthwhile.

(10) All reentry vehicles can be classified in two broad groups--they can have a lift/drag ratio other than zero or no lift at all. The selection of a design largely depends on the vehicle's mission, as well as other factors. One of the most promising configurations is that of the variable-lift/drag-ratio vehicle. Here the value of the lift can be modified to gain maximum benefit of velocity, air density and other similar variables. It may thus be possible to improve on the control and guidance of the vehicle and to reduce the hazards of deceleration and heating as well.

BIBLIOGRAPHY

Federal Government Sources

Department of the Air Force, Air Force Cambridge Research Center:

1. Minzner, R.A. The ARDC Model Atmosphere 1959. AFCRC TR-59-267, August 1959.

Department of the Army, Army Ballistic Missile Agency:

2. An Evaluation of the Radioactive-type Ablation Meter from Cook Electric Company. Report No. DSN-TM-1-58, 5 June 1958, Confidential.

3. Reentry Studies. Vol. I, 25 November 1958, Secret. Vol. II, 31 December 1959, Secret.

4. Bean, K.E. Preliminary Differential Thermal Analysis of Reinforced Plastics. ABMA Report No. DS-TN-113, 28 October 1957, Confidential.

5. _____. Thermal Conductivity and Specific Heat of Three Reinforced Plastic Materials. ABMA Report No. DS-TN-115, 29 October 1957, Confidential.

6. Gray, C.O., and Uptagraft, F. Evaluation of Response of Nose Cone Thermal Insulation Material of Jupiter Missile AM-18 to Reentry Conditions. ABMA Report No. DSN-TM-13-59, 2 October 1959, Secret.

7. Holmes, C.M. The Development of an RF Transparent, Thermal Insulation for the Jupiter Nose Cone. ABMA Report No. DSN-TR-3-59, 5 October 1959, Secret.

8. Johnson, J.S. An Evaluation of Ablation Probes from Detroit Control. ABMA Report No. DSN-TM-11-59, 1 September 1959, Confidential.

9. Kingsbury, J.E. A Comparative Evaluation of the Ablation Characteristics of Goodyear Aircraft Materials P-3010 and XP-132 with P-3000. ABMA Report No. DSN-TM-6-59, 28 May 1959, Confidential.

10. Kingsbury, J. E. An Investigation of Cincinnati Testing Laboratory Second Generation Ablation Materials. ABMA Report No. DSN-TM-7-59, 12 June 1959, Secret.

11. _____. An Investigation of Cincinnati Testing Laboratory Second Generation Ablation Materials Using Asbestos. ABMA Report No. DSN-TM-12-59, 3 September 1959, Secret.

12. _____. Comparison of Cincinnati Testing Laboratory Material CT-301 with CT-326 and Investigation of Tape-Wrap CT-365. ABMA Report No. DSN-TM-5-59, 29 April 1959, Confidential.

13. _____. Considerations of the Pershing Nose Cone Materials. ABMA Report No. DSN-TN-15-58, 8 December 1958, Confidential.

14. _____. Evaluation of Goodyear Aircraft Corporation Nose Cones Employing Various Finishes on the Reinforcement Material. ABMA Report No. DSN-TM-3-59, 13 March 1959, Secret.

15. Lucas, W.R., and Uptagraft, F. Preliminary Evaluation: Response of Nose Cone Thermal Insulation Material of Jupiter Missile AM-5 to Reentry Conditions. ABMA Report No. DSN-TM-5-58, 23 July 1958, Secret.

16. Lucas, W.R., Uptagraft, F., and Nunnelly, J.R. Evaluation Response of Nose Cone Thermal Insulation Material of Jupiter Missile AM-6 to Reentry Conditions. ABMA Report DSN-TM-8-58, 26 November 1958, Secret.

17. Uptagraft, F. An Evaluation of Ablation Characteristics of Goodyear Aircraft Corporation Material P-3010 Applied to the Jupiter Missile Nose Cone Cap. ABMA Report No. DSN-TM-10-59, 28 August 1959, Confidential.

18. _____. Comparison of Ablation Characteristics of Goodyear Aircraft Corporation Materials P-3000 and P-3010 in the Frustrum of Jupiter "C" Test Models. ABMA Report No. DSN-TM-4-59, 22 April 1959, Secret.

19. _____. Evaluation of Goodyear Aircraft Corporation Nose Cone Models Exposed to the Exhaust Jet of the Jupiter Power Plant. ABMA Report No. DSN-TM-1-59, 28 January 1959, Secret.

Department of the Navy, Bureau of Aeronautics, Technical Information Branch:

20. Sanger, E., and Bredt, J. "A Rocket Drive for Long Range Bombers." Translation CGD-32, 1944.

National Advisory Committee for Aeronautics:

21. Allen, H. J. Motion of a Ballistic Missile Angularly Misaligned with the Flight Path Upon Entering the Atmosphere and Its Effect Upon Aerodynamic Heating, Aerodynamic Loads, and Miss Distance. NACA TN 4048, October 1957.

22. Allen, H. J., and Eggers, A. J. A Study of the Motion and Aerodynamic Heating of Ballistic Missiles Entering the Earth's Atmosphere at High Supersonic Speeds. NACA Report 1381, 1958.

23. Callaghan, E.E. An Estimate of the Fluctuating Surface Pressures Encountered in the Reentry of a Ballistic Missile. NACA-TN-4315, July 1958.

24. Chapman, D.R. A Theoretical Analysis of Heat Transfer in Regions of Separated Flow. NACA-TN-3792, October 1956.

25. Eggers, A. J., Allen, H. J., and Neice, S. E. A Comparative Analysis of the Performance of Long-Range Hypervelocity Vehicles. NACA Report 1382, 1958.

26. Eggers, J. A., Hansen, C. F., and Cunningham, B. E. Stagnation-Point Heat Transfer to Blunt Shapes in Hypersonic Flight, Including Effects of Yaw. NACA TN-4229, April 1958.

27. Penland, J. A., and Armstrong, W. O. "Preliminary Aerodynamic Data Pertinent to Manned Satellite Reentry Configurations." NACA RML 58E13a, 21 July 1958, Confidential.

28. Reshotko, E., and Cohen, C. B. Heat Transfer at the Forward Stagnation Point of Blunt Bodies. NACA TN-3513, July 1955.

29. Roberts, L. A Theoretical Study of Stagnation Point Ablation. NACA TN 4392, September 1958

30. Rubesin, M. W., and Inouye, M. A. A Theoretical Study of the Effect of Upstream Transpiration Cooling on the Heat Transfer and Skin-Friction Characteristics of a Compressible Laminar Boundary Layer. NACA TN 3969, 1957.

National Aeronautics and Space Administration:

31. Anderson, M.S., Trussell, D.H., and Stroud, C.W. Research on Radiation Heat Shields for Bodies and Leading Edges. NASA TM X-312, September 1960, Confidential.

32. Armstrong, W.O. Effect of Various Forebody Modifications on the Static Longitudinal Stability and Control Characteristics of a Reentry Capsule at a Mach Number of 9.6. NASA TM X-469, April 1961, Confidential.

33. _____. Hypersonic Aerodynamic Characteristics of Several Series of Lifting Bodies Applicable to Reentry Vehicle Design. NASA TM X-536, June 1961, Confidential.

34. Armstrong, W.O., Stainback, P.C., and McClellan, C.H. The Aerodynamic-Force and Heat-Transfer Characteristics of Lifting Reentry Bodies. NASA TM X-352, August 1960, Confidential.

35. Assadourian, A., and Cheatham, D.C. Longitudinal Range Control During the Atmospheric Phase of a Manned Satellite Reentry. NASA TN D-253, May 1960.

36. Baradell, D.L., and Bertram, M.H. The Blunt Plate in Hypersonic Flow. NASA TN D-408, October 1960.

37. Bird, J.D., and Llewellyn, C.P. An Analysis of the Stability of Spinning Disks During Atmospheric Reentry. NASA TM X-248, March 1960, Confidential.

38. Bird, J.D., and Wolhart, W.D. An Analysis of the Stability and Control of Ballistic Supersonic Impact Reentry Bodies. NASA TM X-198, March 1960, Confidential.

39. Blanchard, W.S., Jr., and Hoffman, S. Effects of Nose Corner Radii, Afterbody Section Deflections, and a Drogue Chute on Subsonic Motions of Manned-Satellite Models in Reentry Configuration. NASA TN D-223, March 1960.

40. Bland, W.M., and Coolie, K.A. Free-Flight Aerodynamic-Heating Data to Mach Number 10.4 for a Modified Von Karman Nose Shape. NASA TN D-889, May 1961.

41. Boissevain, A. G. The Effect of Lateral and Longitudinal-Range Control on Allowable Entry Conditions for a Point Return from Space. NASA TN D-1067, July 1961.

42. Boskenbom, A. S. Graphical Trajectory Analysis. NASA TN D-64, December 1959.

43. Bowman, G. H., and Savin, R. C. An Experimental Investigation in an Atmosphere Entry Simulator of Nylon as an Ablative Material for Ballistic Missiles. NASA TM X-114, December 1959.

44. Bray, R. S., Drinkwater, F. J., III, and White, M. D. A Flight Study of a Power-Off Landing Technique Applicable to Reentry Vehicles. NASA TN D-323, July 1960.

45. Brinich, P. F. Recovery Temperature, Transition, and Heat-Transfer Measurements at Mach 5. NASA TN D-1047, August 1961.

46. Chapman, D. R. An Analysis of the Corridor and Guidance Requirements for Supercircular Entry into Planetary Atmospheres. NASA TR R-55, 1960.

47. _____. An Approximate Analytical Method for Studying Entry into Planetary Atmospheres. NASA TR R-11, 1959.

48. Chapman, D. R., and Kapphahn, A. K. Tables of Z Functions for Atmosphere Entry Analyses. NASA TR R-106, 1961.

49. Cheatham, D. C. A Concept of a Manned Satellite Reentry Which is Completed with a Glide Landing. NASA TM X-226, December 1959, Confidential.

50. Cheatham, D. C., Young, J. W., and Eggleston, J. M. The Variation and Control of Range Traveled in the Atmosphere by a High-Drag Variable-Lift Entry Vehicle. NASA TN D-230, March 1960.

51. Clark, F. L., and Evans, J. M. Some Aerodynamic and Control Studies of Lifting Reentry Configurations at Angles of Attack up to 90° at a Mach Number of 2.91. NASA TM X-338, November 1960.

52. Cleary, J. W. The Effects of Nose Bluntness on the Flow Separation and Longitudinal Characteristics of Ellipsoidal-Nosed Cylinder-Flare Models at Transonic Speeds. NASA TM X-370, August 1960.

53. Compton, D. L. Free-Flight Measurements of Drag and Static Stability for Blunt-Nosed 10° Half-Angle Cone at Mach Number 15. NASA TM X-507, April 1961.

54. Conti, R. J. Approximate Temperature Distributions and Streamwise Heat Conduction Effects in the Transient Aerodynamic Heating of Thin-Skinned Bodies. NASA TN D-895, September 1961.

55. Davidson, R. M., Cheatham, D. C., and Kaylor, J. T. Manual-Control Simulation Study of a Non-Lifting Vehicle During Orbit, Retro-Rocket Firing, and Reentry into the Earth's Atmosphere. NASA TM X-359, September 1960.

56. Davy, W. C., and Seiff, A. A Study of the Stability and Performance of Some Unsymmetrical Truncated Conical Configurations for Lifting Reentry. NASA TM X-504, May 1961, Confidential.

57. Demele, F. A., and Lazzeroni, F. A. Effects of Control Surfaces on the Aerodynamic Characteristics of a Disk Reentry Shape at Large Angles of Attack and Mach Number of 3.5. NASA TM X-576, August 1961, Confidential.

58. Deveikis, W. D., and Walker, R. W. Local Aerodynamic Heat Transfer and Boundary-Layer Transition on Roughened Sphere-Ellipsoid Bodies at Mach Number 3.0. NASA TN D-907, August 1961.

59. Eggers, A. J., Jr., and Wong, T. J. "Reentry and Recovery of Near-Earth Satellites, with Particular Attention to Manned Vehicle." NASA Memo 10-2-58A, October 1958, Confidential.

60. Eggleston, J. M., Baron, S., and Cheatham, D. C. Fixed-Base Simulation Study of a Pilot's Ability to Control a Winged-Satellite Vehicle During High-Drag Variable-Lift Entries. NASA TN D-228, April 1960.

61. Eggleston, J. M., and Young, J. W. Trajectory Control for Vehicles Entering the Earth's Atmosphere at Small Flight-Path Angles. NASA TR R-89, 1961, Confidential.

62. Ellis, M. C., and Huber, P. W. Radio Transmission Through the Plasma Sheath Around a Lifting Reentry Vehicle. NASA TN D-507, January 1961.

63. Everhart, P. E., and Lindsey, W. F. Observations on the Flows Past Blunt Bodies at Transonic Speeds. NASA TM X-169, June 1960, Confidential.

64. Fletcher, H. S. Damping in Pitch and Static Stability of Blunt Cone-Cylinder-Flare Models and Manned Reentry Capsule Models for Various Angles of Attack at a Mach Number of 2.91. NASA TM X-539, July 1961, Confidential.

65. _____. The Damping in Pitch and Static Stability of Six Supersonic-Impact Ballistic Configurations and Three High-Drag Reentry Capsules at a Mach Number of 6.83. NASA TM X-349, January 1961, Confidential.

66. Fletcher, H. S., and Wolhart, W. D. Damping in Pitch and Static Stability of Supersonic Impact Nose Cones, Short Blunt Subsonic Impact Nose Cones, and Manned Reentry Capsules at Mach Numbers from 1.93 to 3.05. NASA TM X-347, November 1960, Confidential.

67. Foster, G. V. Effect of Longitudinal and Lateral Controls on Aerodynamic Characteristics of a Winged Reentry Configuration at a Mach Number of 1.97 and Angles of Attack up to Approximately 90°. NASA TM X-449, February 1961, Confidential.

68. _____. Exploratory Investigation at Mach Number of 2.01 of the Longitudinal Stability and Control Characteristics of a Winged Reentry Configuration. NASA TM X-178, December 1958, Conf.

69. _____. Longitudinal Aerodynamic Characteristics at a Mach Number of 1.97 of a Series of Related Winged Reentry Configurations for Angles of Attack from 0° to 90°. NASA TM X-461, March 1961, Confidential.

70. Foudriat, E. C. Study of the Use of Terminal Controller Technique for Reentry Guidance of a Capsule-Type Vehicle. NASA TN D-828, May 1961.

71. Fournier, P. G. Aerodynamic Characteristics at Low Speed of a Reentry Configuration Having Rigid Retractable Conical Lifting Surfaces. NASA TN D-622, November 1960.

72. Fournier, P.G. Wind-Tunnel Investigation at High Subsonic Speed of the Static Longitudinal Stability Characteristics of a Winged Reentry Vehicle Having a Large Negatively Deflected Flap-Type Control Surface. NASA TM X-179, December 1959.

73. Fuller, F.B. Numerical Solutions for Supersonic Flow of an Ideal Gas Around Blunt Two-Dimensional Bodies. NASA TN D-791, July 1961.

74. Grant, F.C. Analysis of Low-Acceleration Lifting Entry from Escape Speed. NASA TN D-249, June 1960.

75. _____. Importance of the Variation of Drag with Lift in Minimization of Satellite Entry Acceleration. NASA TN D-120, October 1959.

76. _____. Modulated Entry. NASA TN D-452, August 1960.

77. Grier, N.T., and Sands, N. Regime of Frozen Boundary Layers in Stagnation Region of Blunt Reentry Bodies. NASA TN D-865, May 1961.

78. Grimaud, J.E. Wind-Tunnel Investigation at Mach Number 2.91 of Stability and Control Characteristics of Three Lifting Reentry Configurations at Angles of Attack up to 90°. NASA TM X-455, March 1961.

79. Hamaker, F.M. The Ames Atmosphere Entry Simulator and Its Application to the Determination of Ablative Properties of Materials for Ballistic Missiles. NASA TM X-394, October 1960, Confidential.

80. Hansen, C.F. Approximations for the Thermodynamic and Transport Properties of High-Temperature Air. NASA TR R-50, 1959.

81. Hansen, C.F., Early, R.A., Alzofon, F.E., and Witteborn, F.C. Theoretical and Experimental Investigation of Heat Conduction in Air, Including Effects of Oxygen Dissociation. NASA TR R-27, 1959.

82. Harman, R.W., and Boatright, W.B. Investigation of the Aerodynamic Characteristics of a Reentry Capsule with Various Nose Shapes at a Mach Number of 2.91, Including Studies of Nose Spikes as a Means of Control. NASA TM X-426, January 1961, Confidential.

83. Harry, D.P., and Friedlander, A.L. An Analysis of Errors and Requirements of an Optical Guidance Technique for Approaches to Atmospheric Entry with Interplanetary Vehicles. NASA TR R-102, 1961.

84. Hastings, E.C., Curry, T.B., and Dickens, W.L. Stability and Drag Characteristics of Two Low-Drag Reentry Bodies Obtained with Free-Flight Models at Mach Numbers Between 0.96 and 3.28. NASA TM X-243, March 1960, Confidential.

85. Henderson, A., Jr. Investigation of the Flow Over Simple Bodies at Mach Numbers of the Order of 20. NASA TN D-449, Aug. 1960.

86. Hilton, D.A., Mayes, W.H., and Hubbard, H.H. Noise Considerations for Manned Reentry Vehicles. NASA TN D-450, September 1960.

87. Houbolt, J.C., and Batterson, S.A. Some Landing Studies Pertinent to Glider-Reentry Vehicles. NASA TN D-448, August 1960.

88. Howe, J.T. Radiation Shielding of the Stagnation Region by Transpiration of an Opaque Gas. NASA TN D-329, Sept. 1960.

89. _____. Shielding of Partially Reflecting Stagnation Surfaces Against Radiation by Transpiration of an Absorbing Gas. NASA TR R-95, 1961.

90. Huang, S.S. Some Dynamical Properties of the Natural and Artificial Satellites. NASA TN D-502, September 1960.

91. Jackson, C.M., and Harris, R.V. Static Longitudinal Stability and Control Characteristics at Mach Number of 1.99 of a Lenticular-Shaped Reentry Vehicle. NASA TN D-514, October 1960.

92. Jaquet, B.M. Dynamic Stability and Dispersion of a Project Mercury Test Capsule upon Entering the Atmosphere with Effects of Roll Rate, Center-of-Gravity Displacement, and Threshold of a Rate Reaction Control System. NASA TM X-350, January 1961, Confidential.

93. _____. Static Longitudinal and Lateral Stability Characteristics at a Mach Number of 3.11 of Square and Circular Plan-Form Reentry Vehicles, with Some Effects of Controls and Leading-Edge Extensions. NASA TM X-272, May 1960, Confidential.

94. Johnson, J. L., Jr., and Boisseau, P. C. Low Subsonic Measurements of the Static Stability and Control and Oscillatory Stability Derivatives of a Proposed Reentry Vehicle Having an Extensible Heat Shield for High-Drag Reentry. NASA TN D-892, August 1961.

95. Judd, J. H., and Woodbury, G. E. Free-Flight Tests to a Mach Number of 1.5 of Slender Triangular Pyramid Reentry Configurations. NASA TM X-437, March 1961, Confidential.

96. Julius, J.D. Measurements of Pressure and Local Heat Transfer on a 20° Cone at Angles of Attack up to 20° for a Mach Number of 4.95. NASA TN D-179, December 1959.

97. Kenyon, G. C., and Edwards, G. G. A Preliminary Investigation of Modified Blunt 13° Half-Cone Reentry Configurations at Subsonic Speeds. NASA TM X-501, March 1961, Confidential.

98. Kenyon, G. C., and Sutton, F. B. The Longitudinal Aerodynamic Characteristics of a Reentry Configuration Based on a Blunt 13° Half-Cone at Mach Numbers to 0.92. NASA TM X-571, July 1961, Confidential.

99. Kroll, W. D. "Aerodynamic Heating and Fatigue." NASA Memo 6-4-59W, June 1959.

100. Ladson, C. L. Directional and Lateral Stability Characteristics of a Winged Reentry Vehicle at Hypersonic Speeds. NASA TM X-550, August 1961, Confidential.

101. Ladson, C. L., and Johnston, P. J. Aerodynamic Characteristics of a Blunt-Nosed Winged Reentry Vehicle at Supersonic and Hypersonic Speeds. NASA TM X-357, February 1961, Confidential.

102. _____. Aerodynamic Characteristics of Two Winged Reentry Vehicles at Supersonic and Hypersonic Speeds. NASA TM X-346, February 1961, Confidential.

103. Lawson, W. A., McDearmon, R. W., and Rainey, R. W. Investigation of the Pressure Distribution on Reentry Nose Shapes at Mach Number of 3.55. NASA TM X-244, April 1960, Confidential.

104. Lazzeroni, F. A. Aerodynamic Characteristics of Two Disk Reentry Configurations at a Mach Number of 2.2. NASA TM X-567, May 1961, Confidential.

105. Leonard, R. W., Brooks, G. W., and McComb, H. G. Structural Considerations of Inflatable Reentry Vehicles. NASA TN D-457, September 1960.

106. Levy, L. L., Jr. An Approximate Analytical Method for Studying Atmosphere Entry of Vehicles With Modulated Aerodynamic Forces. NASA TN D-319, October 1960.

107. Lichtenstein, R. H. Analytical Investigation of the Dynamic Behavior of a Nonlifting Manned Reentry Vehicle. NASA TN D-416, September 1960, Confidential.

108. Lichtenstein, J. H., and Carney, T. M. Analytical Investigation of an Acceleration Autopilot for Control of the Impact Point of a Ballistic Missile During Reentry. NASA TM X-515, April 1961, Confidential.

109. Lieblein, S. Analysis of Temperature Distribution and Radiant Heat Transfer Along a Rectangular Fin of Constant Thickness. NASA TN D-196, November 1959.

110. Low, G. M. Nearly Circular Transfer Trajectories for Descending Satellites. NASA TR R-3, 1959.

111. Luidens, R. W. Approximate Analysis of Atmospheric Entry Corridors and Angles. NASA TN D-590, January 1961.

112. McFall, J. C. Free-Flight Drag Measurements of Rocket-Boosted Models of Two Reentry Body Configurations at Mach Numbers from 4.3 to 0.6. NASA TM X-118, October 1959, Confidential.

113. McGehee, J. R., and Hathaway, M. E. Landing Characteristics of a Reentry Capsule with a Torus-Shaped Air Bag for Load Alleviation. NASA TN D-628, November 1960.

114. Matting, F. W., Chapman, D. R., Nyholm, J. R., and Thomas, A. G. Turbulent Skin Friction at High Mach Numbers and Reynolds Numbers in Air and Helium. NASA TR R-82, 1960.

115. Mayhue, R. J. Free Flight Measurements of the Base Pressures and Drag of a Flare-Stabilized Cylindrical Reentry Body with an Elliptical Blunt Nose at Mach Numbers from 1.9 to 0.7. NASA TM X-309, September 1960, Confidential.

116. Mayhue, R. J., and Blanchard, W. S. Free Flight Investigation of the Base Pressure and Drag of a Flare-Stabilized Blunt-Nose Reentry Body Having a Fineness Ratio of 3.11 at Mach Numbers from 0.70 to 1.90. NASA TM X-214, March 1960, Confidential.

117. Moeckel, W. E. Departure Trajectories for Interplanetary Vehicles. NASA TN D-80, November 1959.

118. _____. Trajectories with Constant Tangential Thrust in Central Gravitational Fields. NASA TR R-53, 1960.

119. Morris, O. A., and Keith, A. L., Jr. Experimental Investigation of Pressure Distribution and Static Aerodynamic Characteristics for Three Supersonic-Impact Ballistic Reentry Shapes at Mach Numbers of 1.93, 2.55, and 3.05. NASA TM X-453, March 1961, Confidential.

120. Mugler, J. P., Jr., and Olstad, W. B. Static Longitudinal Aerodynamic Characteristics at Transonic Speeds of a Blunted Right Triangular Pyramidal Lifting Reentry Configuration for Angles of Attack up to 110°. NASA TN D-797, June 1961.

121. _____. Static Longitudinal Aerodynamic Characteristics at Transonic Speeds of a Lenticular-Shaped Reentry Vehicle. NASA TM X-423, December 1960, Confidential.

122. Nielsen, J. N., Goodwin, F. K., and Mersman, W. A. "Three-Dimensional Orbits of Earth Satellites Including Effects of Earth Oblateness and Atmospheric Rotation." NASA Memo 12-4-58A, December 1958.

123. Olstad, W. B., Mugler, J. P., Jr., and Cahn, M. S. Static Longitudinal and Lateral Characteristics of a Right Triangular Pyramidal Lifting Reentry Configuration at Transonic Speeds. NASA TN D-655, April 1961.

124. O'Neal, R. L. and Rabb, L. Heat-Shield Performance During Atmospheric Entry of Project Mercury Research and Development Vehicle. NASA TM X-490, May 1961.

125. Page, W.A., Canning, T.N., Craig, R.A., and Stephenson, J.D. Measurements of Thermal Radiation of Air from the Stagnation Region of Blunt Bodies Traveling at Velocities up to 31,000 Feet per Second. NASA TM X-508, June 1961, Confidential.

126. Paulson, J.W., Shanks, R.E., and Johnson, J.L., Jr. Low-Speed Flight Characteristics of Reentry Vehicles of the Glide-Landing Type. NASA TM X-331, September 1960, Confidential.

127. Pearson, A.O. Wind-Tunnel Investigation at Mach Numbers from 0.20 to 1.17 of the Static Aerodynamic Characteristics of a Possible Reentry Capsule. NASA TM X-262, March 1960, Conf.

128. _____. Wind Tunnel Investigation at Mach Numbers from 0.40 to 1.20 of the Static Aerodynamic and Control Characteristics of a Model of a Nonlifting Reentry Capsule in Combination with a Rocket Booster. NASA TM X-317, September 1960, Confidential.

129. _____. Wind-Tunnel Investigation at Mach Numbers from 0.6 to 1.2 of the Static Aerodynamic Characteristics of a Model of a Possible Nonlifting Reentry Capsule in Combination with a Rocket Booster. NASA TM X-318, September 1960, Confidential.

130. Penland, J.A., and Armstrong, W.O. Static Longitudinal Aerodynamic Characteristics of Several Wing and Blunt-Body Shapes Applicable for Use as Reentry Configurations at a Mach Number of 6.8 and Angles of Attack up to 90°. NASA TM X-65, October 1959, Confidential.

131. Petynia, W.W. Model Investigation of Water Landing of a Winged Reentry Configuration Having Outboard Folding Wing Panels. NASA TM X-62, December 1959, Confidential.

132. Phillips, W.H. Research on Blunt-Faced Configurations at Angles of Attack Between 60° and 90°. NASA TM X-315, September 1960, Confidential.

133. Polhamus, E.C., and Geller, E.W. Pressure and Force Characteristics of Noncircular Cylinders as Affected by Reynolds Number with a Method Included for Determining the Potential Flow about Arbitrary Shapes. NASA TR R-46, 1959.

134. Rainey, R.W. Summary of Aerodynamic Characteristics of Low-Lift-Drag-Ratio Reentry Vehicles from Subsonic to Hypersonic Speeds. NASA TM X-588, September 1961, Confidential.

135. Rainey, R. W. Working Charts for Rapid Prediction of Force and Pressure Coefficients on Arbitrary Bodies of Revolution by Use of Newtonian Concepts. NASA TN D-176, December 1959.

136. Rainey, R. W., and Close, W. H. Studies of Stability and Control of Winged Reentry Configurations. NASA TM X-327, September 1960, Confidential.

137. Rakich, J. V. Supersonic Aerodynamic Performance and Static-Stability Characteristics of Two Blunt-Nosed Modified 13° Half-Cone Configurations. NASA TM X-375, September 1960, Confidential.

138. Rashis, B. Exploratory Investigation of Transpiration Cooling of a 40° Double Wedge Using Nitrogen and Helium as Coolants at Stagnation Temperatures from 1,295°F to 2,910°F. NASA TN D-721, May 1961.

139. Rashis, B., and Hopko, R. N. Analytical Investigation of Ablation. NASA TM X-300, June 1960, Confidential.

140. Rashis, B., and Walton, T. E. An Experimental Investigation of Ablating Materials at Low and High Enthalpy Potentials. NASA TM X-263, March 1960, Confidential.

141. Reller, J. O. Heat Transfer to Blunt Axially Symmetric Bodies. NASA TM X-391, September 1960, Confidential.

142. Reller, J. O., and Seegmiller, H. L. Convective Heat Transfer to a Blunt Lifting Body. NASA TM X-378, September 1960, Confidential.

143. Roberts, L. An Analysis of Ablation-Shield Requirements for Manned Reentry Vehicles. NASA TR R-62, 1960.

144. _____. An Analysis of Nose Ablation for Ballistic Vehicles. NASA TN D-254, April 1960.

145. _____. Stagnation Point Shielding by Melting and Vaporization. NASA TR R-10, 1959.

146. Robinson, R. B., and Spearman, M. L. Stability and Control Characteristics at a Mach Number of 1.89 of a Lightweight Glider Reentry Configuration. NASA TM X-276, May 1960, Confidential

147. Rumsey, C.B., and Lee, D.B. Heat Transfer Measurements on a Blunt Spherical-Segment Nose to a Mach Number of 15.1 and Flight Performance of the Rocket-Propelled Model to a Mach Number of 17.8. NASA TM X-77, November 1959, Confidential.

148. Rumsey, C.B., Piland, R.O., and Hopko, R.N. Aerodynamic-Heating Data Obtained from Free-Flight Tests Between Mach Numbers of 1 and 5. NASA TN D-216, January 1960.

149. Sarabta, M.F. Aerodynamic Characteristics of a Blunt Half-Cone Entry Configuration at Mach Numbers from 3 to 6. NASA TM X-393, October 1960, Confidential.

150. Savin, R.C., Gloria, H.R., and Dahms, R.G. Ablative Properties of Thermoplastics under Conditions Simulating Atmosphere Entry of Ballistic Missiles. NASA TM-397, November 1960, Confidential.

151. Scallion, W.I. Full-Scale Wind-Tunnel Investigation of the Low-Speed Static Aerodynamic Characteristics of a Model of a Re-entry Capsule. NASA TM X-220, October 1959, Confidential.

152. Shaw, D.S., and Turner, K.L. Wind-Tunnel Investigation of Static Aerodynamic Characteristics of a 1/9-Scale Model of a Possible Reentry Capsule at Mach Numbers from 2.29 to 4.65. NASA TM X-233, December 1959, Confidential.

153. Slye, R.E. An Analytical Method for Studying the Lateral Motion of Atmosphere Entry Vehicles. NASA TN D-325, September 1960.

154. Smith, D.W., and Walker, J.H. Skin Friction Measurements in Incompressible Flow. NASA TR R-26, 1959.

155. Smith, F.M., and Nichols, F.H. A Wind-Tunnel Investigation of the Aerodynamic Characteristics of a Generalized Series of Winged Reentry Configurations at Angles of Attack to 180° at Mach Numbers of 2.38, 2.99 and 4.00. NASA TM X-512, June 1961, Confidential.

156. Smith, O.E., and Chenoweth, H.B. Range of Density Variability from Surface to 120 KM Altitude. NASA TN D-612, July 1961.

157. Smith, W.G. A Wind-Tunnel Investigation at Subsonic and Low Supersonic Speeds of a Reentry Vehicle with Retractable Wings. NASA TM X-398, February 1961, Confidential.

158. Sommer, S.C., Short, B.J., and Compton, D.L. Free-Flight Measurements of Static and Dynamic Stability of Models of the Project Mercury Reentry Capsule at Mach Numbers 3 and 9.5. NASA TM X-373, August 1960, Confidential.

159. Sparrow, E.M. Unsteady Stagnation-Point Heat Transfer. NASA TN D-77, October 1959.

160. Spencer, B. An Investigation at Subsonic Speeds of Aerodynamic Characteristics at Angles of Attack from -4° to 100° of a Delta-Wing Reentry Configuration Having Folding Wingtip Panels. NASA TM X-288, May 1960, Confidential.

161. _____. An Investigation at Subsonic Speeds of the Longitudinal Aerodynamic Characteristics at Angles of Attack from -4° to 100° of Delta-Wing Reentry Configurations Having Vertically Displaced and Cambered Wingtip Panels. NASA TM X-440, February 1961, Confidential.

162. _____. An Investigation of the Aerodynamic Characteristics at Subsonic Speeds of a Nonlifting-Type Space-Capsule Model Simulating Escape and Reentry Configurations. NASA TM X-228, March 1960, Confidential.

163. Stainback, P.C. Visual Technique for Determining Qualitative Aerodynamic Heating Rates on Complex Configurations. NASA TN D-385, October 1960.

164. Stephens, E.W. Afterbody Heating Data Obtained from an ATLAS-Boosted MERCURY Configuration in a Free Body Reentry. NASA TM X-493, August 1961, Confidential.

165. Swann, R.T., and South, J. A Theoretical Analysis of Effects of Ablation on Heat Transfer to an Arbitrary Axisymmetric Body. NASA TN D-741, April 1961.

166. Swenson, B.L. A Study of Methods for Simulating the Atmosphere Entry of Vehicles with Small-Scale Models. NASA TN D-90, April 1960.

167. Swenson, B. L. Exploratory Study of the Reduction in Friction Drag Due to Streamwise Injection of Helium. NASA TN D-342, January 1961.

168. Tendeland, T. Effects of Mach Number and Wall-Temperature Ratio on Turbulent Heat Transfer at Mach Numbers from 3 to 5. NASA TR R-16, 1959.

169. Terry, J.E. Convective Heat Transfer to a Lifting Flat-Faced-Cone Entry Body. NASA TM X-509, May 1961, Confidential.

170. Trescot, C.D., and Putnam, L.E. Low-Speed Full-Scale Reynolds Number Investigation of the Effects of Wing Leading-Edge Radius Elevons, Landing Gear, and a Body Flap on the Static Longitudinal Aerodynamic Characteristics of a Winged Reentry Configuration. NASA TM X-553, August 1961, Confidential.

171. Tunnell, P. J. The Static and Dynamic Stability Derivatives of a Blunt Half-Cone Entry Configuration at Mach Numbers from 0.70 to 3.50. NASA TM X-577, August 1961, Confidential.

172. Van Dyke, M. D., and Gordon, H. D. Supersonic Flow Past a Family of Blunt Axisymmetric Bodies. NASA TR R-1, 1959.

173. Vaughan, V. L., Jr. Landing Characteristics and Floatation Properties of a Reentry Capsule. NASA TN D-653, February 1961.

174. _____. Water Landing Impact Accelerations for Three Models of Reentry Capsules. NASA TN D-145, October 1959.

175. Wagner, R. D., Pine, W. C., and Henderson, A., Jr. Laminar Heat-Transfer and Pressure Distribution Studies on a Series of Reentry Nose Shapes at a Mach Number of 19.4 in Helium. NASA TN D-891, June 1961.

176. Ware, G. M. Low-Subsonic-Speed Static Longitudinal Stability and Control Characteristics of a Winged Reentry-Vehicle Configuration Having Wingtip Panels that Fold Up for High-Drag Reentry. NASA TM X-227, February 1960.

177. _____. Low Subsonic Speed Static Stability of Right-Triangular Pyramid and Half-Cone Lifting Reentry Configurations. NASA TN D-646, February 1961.

178. Ware, G. M. Static Stability and Control Characteristics at Low-Subsonic Speeds of a Lenticular Reentry Configuration. NASA TM X-431, December 1960, Confidential.

179. Wehrend, W. R., and Reese, D. E., Jr. Wind-Tunnel Tests of the Static and Dynamic Stability Characteristics of Four Ballistic Reentry Bodies. NASA TM X-369, June 1960, Confidential.

180. Weston, K. C., and Swanson, J. E. A Compilation of Wind-Tunnel Heat-Transfer Measurements on the Afterbody of the Project Mercury Capsule Reentry Configuration. NASA TM X-495, August 1961, Confidential.

181. White, J. S. A Study of the Guidance of a Space Vehicle Returning to a Breaking Ellipse about the Earth. NASA TN D-191, January 1960.

182. _____. Investigation of the Errors of an Internal Guidance System During a Satellite Reentry. NASA TN D-322, August 1960.

183. Wiley, H. G., Kilgore, R. A., and Hillje, E. R. Dynamic Directional Stability Characteristics for a Group of Blunt Reentry Bodies at Transonic Speeds. NASA TM X-337, October 1960.

184. Wingrove, R. C., and Coate, R. E. Piloted Simulator Tests of a Guidance System Which Can Continuously Predict Landing Point of a Low L/D Vehicle During Atmosphere Reentry. NASA TN D-787, March 1961.

185. Wisniewski, R. J. Methods of Predicting Laminar Heat Rates on Hypersonic Venicles. NASA TN D-201, December 1959.

186. Wong, R. Y., Darmstadt, D. L., and Monroe, D. E. Investigation of a 4.0-Inch-Mean-Diameter Four-Stage Reentry Turbine for Auxiliary Power Drives. NASA TM X-152, March 1960, Confidential.

187. Wong, T. J., Goodwin, G., and Slye, R. E. Motion and Heating During Atmosphere Reentry of Space Vehicles. NASA TN D-334, September 1960.

188. Wong, T. J., and Slye, R. E. The Effect of Lift on Entry Corridor Depth and Guidance Requirements for the Return Lunar Flight. NASA TR R-80, 1961.

189. Young, J. W. A Method for Longitudinal and Lateral Range Control for High-Drag Low-Lift Vehicle Entering the Atmosphere of a Rotating Earth. NASA TN D-954, September 1961.

Nongovernmental Sources

190. Adams, E. W. Theoretical Investigations of the Ablation of a Glass-type Heat Protection Shield of Varied Material Properties at the Stagnation Point of a Reentry IRBM. January 1961.

191. Adams, M. C., Powers, W. E., and Georgie, V. S. "An Experimental and Theoretical Study of Quartz Ablation at the Stagnation Point." Journal of the Aerospace Sciences. Vol. 27, No. 7, July 1960.

192. Avco-Everett Research Laboratory. Reentry Physics Evaluation Program. March 1960.

193. _____. Reentry Physics Program Semi-Annual Technical Summary Report. June 1960.

194. Baron, J. R. Binary Mixture Boundary Layer Associated with Mass Transfer Cooling at High Speeds. Massachusetts Institute of Technology, Naval Supersonic Laboratory. Technical Report No. 160, 1956.

195. Becker, J. V. "Reentry from Space." Scientific American. January 1961.

196. Bernicker, R. P. An Experiment with a Transpiration Cooled Nozzle. Massachusetts Institute of Technology, Naval Supersonic Laboratory. Technical Report No. 447, 1960.

197. Burrows, D. L. Effect of Choice of Temperature for Determining Air Property Values on the Turbulent Heat Transfer on a Sphere. March 1957.

198. Burrows, D. L., McWorter, J. K., and Edwards, J. F. The Correlation of Supersonic Flows on Blunt-Nosed Bodies in Gases of Different Specific Heat Ratios. March 1958.

199. Camm, J. Qualitative Interpretation of Spectra of Jupiter Re-entry. Avco-Everett Research Laboratory. Research Note 96, 30 September 1958.

200. Connell, H. A. A Procedure for Estimating Turbulent Heat Transfer on Round Nose Objects and a Comparison with Certain Flight Cases. August 1957, Secret.

201. _____. Comparison of Theoretical and Experimental Ablation Rates of Fiberglass Re-enforced Plastic. July 1957, Confidential.

202. Connell, H. A., and Burleson, W. G. Comparison on Aerodynamic Heating Simulation Facilities to a Point on a 1500 N. M. Jupiter Trajectory and Certain Flight Data. October 1957, Secret.

203. Convair, San Diego. Reentry Studies. 27 May 1959, Secret.

204. Cooke, C. H., Kivel, B., Lin, S. C., and Petty, C. C. A Note on Radar Return During Reentry. Avco-Everett Research Laboratory. Research Note 187, March 1960, Secret.

205. Cresci, R. J., McKenzie, D. A., and Libby, P. A. "An Investigation of Laminar, Transitional, and Turbulent Heat Transfer on Blunt Nosed Bodies in Hypersonic Flow." Journal of the Aerospace Sciences. Vol. 27, No. 6, June 1960

206. Denison, M. R. "The Turbulent Boundary Layer on Chemically Active Ablating Surfaces." Journal of the Aerospace Sciences. June 1961.

207. Detra, R. W., Kemp, N. H., and Riddell, F. R. "Addendum to Heat Transfer to Satellite Vehicles Reentering the Atmosphere." Jet Propulsion. Vol. 27, No. 12, December 1957.

208. Ehricke, K. A., and Pence, H. "Reentry of Spherical Bodies into the Atmosphere at Very High Speeds." American Rocket Society Preprint 428-57, April 1957.

209. Esses, H. "Satellite Orbit Mechanics." Aerospace Engineering. April 1959.

210. Feldman, S. A Numerical Comparison Between Exact and Approximate Theories of Hypersonic Inviscid Flow Past Slender Blunt-Nosed Bodies. Avco-Everett Research Laboratory. Research Report 71, June 1959.

211. _____. On the Trails of Hypervelocity Blunt Bodies Flying Through the Atmosphere. Avco-Everett Research Laboratory. Research Note 190, January 1960, Secret.

212. _____. Trails of Axi-symmetric Hypersonic Blunt Bodies Flying Through the Atmosphere. Avco-Everett Research Laboratory. Research Paper 82, December 1959.

213. Ferri, A., Feldman, L., and Daskin, W. "The Use of Lift for Reentry from Satellite Trajectories." Jet Propulsion. Vol. 27, No. 11, November 1957.

214. Gaines, L. M., and Surber, T. E. "Prediction of Optimum Approach and Landing Techniques for Manned Reentry Gliders." Institute of Aeronautical Sciences Paper No. 61-115-1809, 1961.

215. Gazley, C. Deceleration and Heating of a Body Entering a Planetary Atmosphere from Space. The RAND Corporation. Report P-955, 18 February 1957.

216. _____. Heat-Transfer Aspects of the Atmospheric Reentry of Long Range Ballistic Missiles. The RAND Corporation. Report No. R-273, 1 August 1954, Confidential.

217. Gazley, C., and Masson, D. J. A Recoverable Scientific Satellite. The RAND Corporation. Report RM-1844, 21 December 1956.

218. Haig, C.R. "The Use of Rotors for the Landing and Reentry Braking of Manned Spacecraft." Institute of Aeronautical Sciences Paper No. 60-17, 25-27 January 1960.

219. Hermann, R. "Reentry Trajectories and Problems of Hypersonic Flow. Space Trajectories. New York: Academic Press, Inc., 1960.

220. The Johns Hopkins University, Applied Physics Laboratory. Reentry Physics for Terminal Defense Against Ballistic Missiles. TG-368, July 1960, Secret, Restricted Data.

221. Kemp, N.H., and Riddell, F.R. "Heat Transfer to Satellite Vehicles Reentering the Atmosphere." Jet Propulsion. Vol. 27, No. 2, February 1957.

222. Kivel, B., and Hidalgo, H. Preliminary Map of Reentry Phenomena. Avco-Everett Research Laboratory. Research Note 124, April 1959, Secret.

223. Kuiper, G.P. The Atmospheres of the Earth and Planets. Rev. ed. Chicago: University of Chicago Press, 1951.

224. Lees, L. "Laminar Heat Transfer over Blunt-Nosed Bodies at Hypersonic Flight Speeds." Jet Propulsion. Vol. 26, No. 4, April 1956.

225. Lees, L., Hartwig, F.W., and Cohen, C.B. The Use of Aerodynamic Lift During Entry into the Earth's Atmosphere. Space Technology Laboratories, Inc. GM-TR-0165-00519, 20 November 1958.

226. Lin, S.C. A Suggestion for Down-Range Observation of the Ionized Wake of Reentry Objects. Avco-Everett Research Laboratory Research Note No. 150, July 1959, Secret.

227. _____. Ionized Wakes of Reentry Objects. Avco-Everett Research Laboratory. Research Note 131, June 1959, Secret.

228. Lin, S.C., and Feldman, S. Note on the Ionized Wake of Reentry Objects. Avco-Everett Research Laboratory. Research Note 168, December 1959, Secret.

229. Loh, W.H.T. "A Second Order Theory of Entry Mechanics into a Planetary Atmosphere." Institute of Aeronautical Sciences Paper No. 61-116-1810, 1961.

230. _____. "Dynamics and Thermodynamics of Reentry." Journal of the Aerospace Sciences. Vol. 27, No. 10, October 1960.

231. Moses, J.L., and Wood, C.C. An Analysis of the Effect of Angle of Attack on the Laminar and Turbulent Heat Transfer Coefficient to the Spherical Nose of a Spinning Missile. November 1957, Confidential.

232. Myers, H. "Aerodynamically Heated Surfaces - A Chemical Analysis." Aerospace Engineering. Vol. 19, No. 2, February 1960.

233. Nagamatsu, H. T., Geiger, R. E., and Sheer, R. E. "Real Gas Effects in Flow Over Blunt Bodies at Hypersonic Speeds." Journal of the Aerospace Sciences. Vol. 27, No. 4, April 1960.

234. Neilsen, J. "Three-Dimensional Satellite Orbits with Emphasis on Reentry Dynamics and Oblateness Effects." Aerospace Engineering. April 1959.

235. Paul, H. G. Nose Cone Reentry Heating for Different Heat Protection Materials. 27 September 1956, Secret.

236. Persh, J. Third Semi-Annual Progress Report on the Status of the Reentry Body Applied Research Programs. 19 January 1959, Confidential.

237. Petty, CC., Hidalgo, H., Keck, J. C., Adams, M. C., and Prescott, R. Avco-Everett Research Laboratory. Avco-Everett Participation in Project Big Arm. 8 April 1960, Secret.

238. The RAND Corporation. An Introduction to Astronautics. Vol. I, 24 February 1958, Secret.

239. RCA Missile and Surface Radar Division. Interim Reentry Data Report - ATLAS Missile 62-D - AMR Test No. 801. 21 July 1960, Secret.

240. _____. Interim Reentry Data Report - TITAN Missile G-10 - AMR Test No. 1802. 26 July 1960, Secret.

241. Romig, M. F. "Stagnation Point Heat Transfer for Hypersonic Flow." Jet Propulsion. Vol. 26, No. 12, December 1956.

242. Sanger, E. Raketen-Flugtechnik. Berlin, 1933.

243. Scala, S. M. "Sublimation in a Hypersonic Environment." Journal of the Aerospace Sciences. Vol. 27, No. 1, January 1960.

244. Scala, S. M., and Diaconis, N. S. "The Stagnation Point Ablation of Telflow During Hypersonic Flight." Journal of the Aerospace Sciences. February 1960.

245. Smith, R.H., and Menard, J.A. "Supercircular Entry and Recovery with Maneuverable Manned Vehicles." Institute of Aeronautical Sciences Paper No. 61-114-1808, 1961.

246. Stehling, K.R. "How Far Are We on Reentry Cooling?" Aerospace Engineering. September 1959.

247. Sutton, G.W. "Ablation of Reenforced Plastics in Supersonic Flow." Journal of the Aerospace Sciences. Vol. 27, No. 5, May 1960.

248. Truitt, R.W. Fundamentals of Aerodynamic Heating. New York: The Ronald Press Company, 1960.

249. Vaglio-Laurin, R. "Turbulent Heat Transfer on Blunt-Nosed Bodies in Two-Dimensional and General Three-Dimensional Hypersonic Flow." Journal of the Aerospace Sciences. January 1960.

250. Wagner, C. The Calculation of the Skin Temperature of Rockets. November 1946.

251. _____. The Density of the Air Around a Wedge and a Cone in an Air Flow of Supersonic Velocity. October 1946.

252. _____. Skin Temperature of Missiles Entering the Atmosphere at Hypersonic Speed. October 1949.

253. Warren, W.R., and Diaconis, N.S. "The Performance of Ablation Materials as Heat Protection for Reentering Satellites." Institute of Aeronautical Sciences Paper No. 60-49, 25-27 January 1960.

254. Welterlen, J. "Aeronautical and Space Applications for Ceramics." Aerospace Engineering. April 1959.

255. Wilson, H.B. Heat Flux, Heat Input, Ablation Weights and Thickness of Fiberglass for Jupiter Top 14, Range 500 to 1500, Ballistic Factors 3.6×10^{-3}, 3.1×10^{-3} and 2.7×10^{-3} $M^3/KGSEC^2$. June 1957, Secret.

256. _____. Some Heat Transfer Computations for Reentry Missile Top. July 1957, Secret.

257. Wilson, H. B. Study of a Fiberglass Coating for the Reentry Missile Top. October 1956, Secret.

258. Wing, L. D. "Evaluation of Thermal Problems at Relatively Low Orbital Altitudes." Aerospace Engineering. March 1960.

259. Wood, R. M., and Tagliani, R. J. "Heat Protection by Ablation." Institute of Aeronautical Sciences Paper No. 60-8, 25-27 January 1960.

260. Yaffee, M. "Ablation Wins Missile Performance Gain." Aviation Week. 18 July 1960.

261. Zartarian, G., Hsu, P. T., and Ashley, H. "Dynamic Airloads and Aeroelastic Problems at Entry Mach Numbers." Institute of Aeronautical Sciences Paper No. 60-32, 25-27 January 1960.

National Aeronautics and Space Administration:

262. Welver, J. E. Comparison of Theoretical and Experimental Valves for the Effective Heat of Ablation of Ammonium Chloride. NASA TN D-553, November 1960.

APPENDIX I

Notation

a	acceleration
$\vec{a}$	acceleration vector
A	area of cross section
c	specific heat
c_1	heat of fusion
C	dimensional constant for stagnation-point heat-transfer rate
c_2	heat of vaporization
C_D	drag coefficient
C_L	lift coefficient
D	drag force
e	basis of a natural logarithm
E	energy
ESC	escape
$\vec{F}$	force vector
g	gravitational acceleration
i	unit vector in the X direction of a Cartesian coordinate system
i_R	unit vector in the R direction
i_θ	unit vector in the θ direction
j	unit vector in the y direction of a Cartesian coordinate system
k	unit vector in the Z direction of a Cartesian coordinate system

k_1 ratio of heat rate (q_{l1}) at a given point on the surface to the heating rate (q_{ls}) at the stagnation point or $k_1 = \frac{q_{l1}}{q_{ls}}$

K_c constant in transpiration cooling equation

L lift force

m mass or rate of mass loss

M total mass in the reentry vehicle

$\overline{M}$ mean molecular weight of atmosphere

P wall-injector parameter

P_r Prandtl number

q_l dynamic pressure

q_{l1} aerodynamic heating rate per unit area

q_{ls} aerodynamic heating rate per unit area at stagnation point

Q total heat absorbed

Q_1 amount of heat absorbed and retained in the ablation shield per unit mass

Q_2 total heat absorbed by the ablation shield per unit mass, or total heat absorbed by the heat sink

r radius (usually distance to the center of the earth)

R radius of curvature of a space-vehicle surface configuration

Re Reynolds number

R_0 radius of earth

S airfoil surface area

SL sea level

t time

T temperature

T_1 temperature of fusion

T_2 reentry temperature

T_{aw} adiabatic wall temperature under zero coolant injection

T_c temperature of the coolant

T_w temperature at the wall

$\overline{T_{ws}}$ stagnation surface temperature

$\overline{T_\infty}$ free-stream atmospheric temperature

V velocity of reentering body

$\overline{V}$ dimensionless variable equal to $\frac{V_1}{V_c}$

V_c circular velocity

V_{ESC} escape velocity

V_1 velocity in the direction of motion or tangential component of circumferential velocity

V_2 velocity vertical to tangential component

W mass of the vehicle in pounds

x distance from stagnation point

x_i distance from stagnation point to start of injection

x_o distance from stagnation point to injection cutoff point

X distance parameter

y altitude

β reciprocal characteristic height of the atmosphere

γ ratio of specific heats

ϵ surface radiative emissivity

θ local flight path angle

θ_E angle of entry into the atmosphere

μ coefficient of viscosity

μ_{SL} coefficient of viscosity at sea level

ρ density

ρ_o a reference atmospheric density frequently taken as equal to ρ_{SL}

ρ_{SL} density at sea level

ρ_y density at altitude y

ρ_∞ free-stream atmospheric density

$(\rho u)_o$ mainstream mass flow per unit area at the injection cutoff point

$(\rho v)_w$ mean injection mass flow per unit area

σ ratio $\frac{\rho}{\rho_{SL}}$

* * * * *

Btu British thermal unit

cep circular probable error

fps feet per second

ICBM intercontinental ballistic missile

psf pounds per square foot